Journal Pre-proof

Purine/purine isoster based scaffolds as new derivatives of benzamide class of HDAC inhibitors

Kunal Nepali, Ting-Yu Chang, Mei-Jung Lai, Kai-Cheng Hsu, Yun Yen, Tony Eight Lin, Sung-Bau Lee, Jing-Ping Liou

PII: S0223-5234(20)30260-9

DOI: https://doi.org/10.1016/j.ejmech.2020.112291

Reference: EJMECH 112291

To appear in: *European Journal of Medicinal Chemistry*

Received Date: 29 November 2019

Revised Date: 17 March 2020

Accepted Date: 27 March 2020

Please cite this article as: K. Nepali, T.-Y. Chang, M.-J. Lai, K.-C. Hsu, Y. Yen, T.E. Lin, S.-B. Lee, J.-P. Liou, Purine/purine isoster based scaffolds as new derivatives of benzamide class of HDAC inhibitors, *European Journal of Medicinal Chemistry* (2020), doi: https://doi.org/10.1016/j.ejmech.2020.112291.

Graphical Abstract

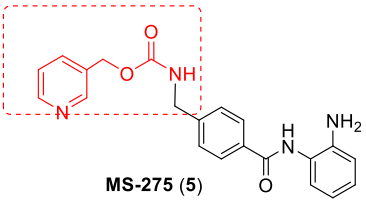

MS-275 (**5**)

IC_{50} (μM) = 2.60 ± 0.16 (MDA-MB-231)
= 4.54 ± 0.21 (HepG2)
= 6.03 ± 0.44 (YCC11, HDACi-sensitive gastric cancer cell lines)
= 12.98 ± 1.02 (YCC3/7, HDACi-resistant gastric cancer cell lines)
= 0.544 (HDAC1)
= 0.613 (HDAC2)
= 0.624 (HDAC3)

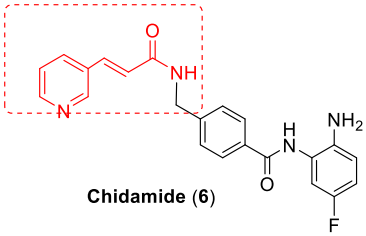

Chidamide (**6**)

IC_{50} (μM) = 3.60 ± 0.36 (MDA-MB-231)
> 8 (HepG2)
= 17.07 ± 1.60 (YCC11, HDACi-sensitive gastric cancer cell lines)
= 20.44 ± 0.38 (YCC3/7, HDACi-resistant gastric cancer cell lines)

⟹

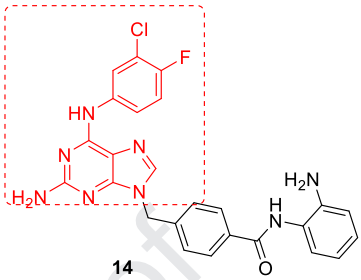

14

IC_{50} (μM) = 1.48 ± 0.06 (MDA-MB-231)
= 2.44 ± 0.18 (HepG2)
= 4.77 ± 0.29 (YCC11, HDACi-sensitive gastric cancer cell lines)
= 4.79 ± 0.37 (YCC3/7, HDACi-resistant gastric cancer cell lines)
= 0.108 (HDAC1)
= 0.585 (HDAC2)
= 0.563 (HDAC 3)

European Journal of Medicinal Chemistry

Purine/Purine isoster based scaffolds as new derivatives of benzamide class of HDAC inhibitors

Kunal Nepali[a,1], Ting-Yu Chang[b,c,d,1], Mei-Jung Lai[c], Kai-Cheng Hsu[b,e,d], Yun Yen[d], Tony Eight Lin[d], Sung-Bau Lee[*,b,c], Jing-Ping Liou[*,a,b,e,f]

[1]These authors contributed equally to this work

*To whom correspondence should be addressed. S. B. Lee: (Phone) 886-2-7361661 ext 6107; (e-mail) sbl@tmu.edu.tw; J. P. Liou: (Phone) 886-2-2736-1661 ext 6130; (e-mail) jpl@tmu.edu.tw

[a] *School of Pharmacy, College of Pharmacy, Taipei Medical University.*
[b] *Ph.D. Program in Biotechnology Research and Development, College of Pharmacy, Taipei Medical University.*
[c] *Master Program in Clinical Pharmacogenomics and Pharmacoproteomics, College of Pharmacy, Taipei Medical University.*
[d] *Graduate Institute of Cancer Molecular Biology and Drug Discovery, College of Medical Science and Technology, Taipei Medical University.*
[e] *TMU Biomedical Commercialization Center, Taipei Medical University.*
[f] *School of Pharmacy, National Defense Medical Center, Taipei, Taiwan*

Abstract: This study reports the design, synthesis and evaluation of a series of histone deacetylase (HDAC) inhibitors containing purine/ purine isoster as a capping group and an N-(2-aminophenyl)-benzamide unit. In vitro cytotoxicity studies reveal that benzamide ***14*** suppressed the growth of triple-negative breast cancer cells MDA-MB-231 (IC_{50} = 1.48 μM), MDA-MB-468 (IC_{50} = 0.65 μM), and liver cancer cells HepG2 (IC_{50} = 2.44 μM), better than MS-275 (**5**) and Chidamide (**6**). Compared to the well-known HDAC inhibitor SAHA, **14** showed a higher toxicity (IC_{50} = 0.33 μM) in three leukemic cell lines, K-562, KG-1 and THP-1. Moreover, **14** was found to be equally virulent in the HDAC-sensitive and -resistant gastric cell lines, YCC11 and YCC3/7, respectively, indicating the potential of **14** to overcome HDACi resistance. Furthermore, substantial inhibitory effects more pronounced than MS-275 (**5**) and Chidamide (**6**) were displayed by **14** towards HDAC1, 2 and 3 isoforms with IC_{50} values of 0.108, 0.585 and 0.563 μM respectively. Compound **14** also exhibited a potent antitumor efficacy in human MDA-MB-231 breast cancer xenograft mouse model, providing a potential lead for the development of anticancer agents.

Key words: Purines, isosters, histone deacetylase inhibitors, drug resistance.

1. Introduction

Epigenetic modification of histones is involved in the regulation of cell-specific expression of genes required for development and maintenance of cellular function [1]. Histone deacetylases (HDAC) induce histone hypoacetylation by removing the acetyl groups on *N*-terminal lysines of histone proteins, which in turn loosens the chromatin structure and ultimately facilitates the transcriptional process [2]. HDACs as drug targets have garnered significant scientific attention [2,3] as HDAC inhibitors induce relief of transcriptional repression in various leukemias and are considered to be the key for epigenetic cancer therapy [4]. Recent literature clearly indicates that there has been an explosion of research on design and synthesis of class I HDAC inhibitors as antiproliferative agents and promising results were attained [5-9]. In this view, class I HDAC inhibition appears to be an attractive therapeutic strategy for developing anticancer agents.

Structural fabrication of HDAC inhibitors includes a cap group (CAP), linker part and a Zn-binding group (ZBG) and HDAC inhibitors are generally categorized in to two structural classes on the basis of the zinc binding group: Hydroxamic acids and the aminoanilides (benzamides). SAHA (**1**) [10], PXD101 (**2)** [11] and LBH589 (**3**) [12] represent the US FDA approved hydroxamic acid type HDAC inhibitors (Fig. 1) and Mocetinosat (**4**) [13], MS-275 (**5**) [14] and Chidamide (**6**) [14] (Fig. 1) are the representative examples of N-(2-Aminophenyl)benzamide binding unit containing HDAC inhibitors. Among the

benzamides, only Chidamide (**6**) stands as the approved benzamide (CFDA approved) for the treatment of patients with recurrent or refractory peripheral T-cell lymphoma (PTCL) [14-17]. In preliminary studies, Mocetinostat (**4**) has also demonstrated significant anticancer efficacy that has been attributed to its slow, tight binding to HDACs and its slow decomplexation [18-19]. In addition, there were no observed signs of acquired resistance of cancer cells towards the exposure to Mocetinostat [20]. Another N-(2-Aminophenyl)benzamide type HDAC inhibitor, MS-275 (**5**) owing to its clinical promise and selective class I inhibitory potential has been the subject of extensive structural engineering with numerous studies yielding optimistic results [21]. These exciting facts clearly ascertains the need of extensive explorations on new aminoanilide inhibitors.

We have been actively involved in the search of small molecule HDAC inhibitors employing diverse combinations of CAP constructs, linker and zinc binding motifs [22]. As an extension of this ongoing drug discovery program, the present study deals with the structural optimization of the MS-275 and Chidamide chemical architecture that involves feasible inclusion of purine/purine isoster as the surface recognition motif and the replacement of the carbamate and acrylamide groups as the connecting unit to the benzyl linker (Fig. 2). These attempts were particularly influenced by the literature rationale of attaining favorable effects via placement of a bicyclic heteroaryl ring as the CAP component in the structural template of MS-275/Chidamide

[21, 23] along with the existence of purine/purine isosters as a key structural unit in the chemical architecture of numerous bioactive scaffolds exerting potent cell killing effects [24]. Other than this, the formation of a toxic metabolite, 4-(aminomethyl)-N-(2-aminophenyl)benzamide which nonspecifically inhibits HDAC proteins or other targets attributed to the presence of carbamate functionality in the structure of MS-275 (Fig. 2) [23] led us conceive that its replacement as the connecting unit can be a logical approach to overcome this issue. Furthermore, the CAP constructs were fused with substituted anilines and heteroaryl amines reported to possess anticancer effects [24]. The fusion of such antitumor pharmacophores is anticipated to induce sensitization of the cancer cells towards the exposure of the designed synthetics. With this background, we describe here the synthesis and preliminary antiproliferative evaluation of a new series of aminoanilides (**7-18**) (Fig. 2) containing purine/purine isoster as the capping group.

2. Results

2.1 Chemistry

Schemes 1-4 presents the synthetic routes to the target benzamides (**7-18**). Benzamides **7**, **11**, **13** and **17** were synthesized as per the synthetic approach shown in scheme 1. Substituted 9H-Purine (**19**, **21**) and 7H-Pyrrolo[2,3-d]pyrimidine (**20**, **22**) were subjected to potassium carbonate mediated benzylation with methyl 4-(bromomethyl)benzoate employing a previously

reported methodology. For the purine based starting materials (**19** and **21**), benzylation proceeded regioselectively towards N-9 position and the results were in resonance with the results of the protocol [25]. The benzylated products **23-26** were hydrolyzed using lithium hydroxide to yield the carboxylic acid (**27-30**). The acids (**27-29**) underwent EDC/HOBt mediated amidation with benzene-1,2-diamine to get the desired benzamides (**7, 11, 13**) while the acid 30 was amide coupled with (2-Amino-4-fluoro-phenyl)-carbamic acid *tert*-butyl ester followed by trifloroacetic acid mediated Boc deprotection to furnish the target benzamide **17**. Scheme 2 depicts the methodology for the preparation of benzamides **8**, **10**, **12**, **14-16**. Protic acid catalyzed condensation of substituted anilines and 4-methyl-2H-pyrazol-3-ylamine with the starting materials **(19-22**) yielded intermediates **31-36.** The intermediates **31-36** were then subjected to the previously employed synthetic route as mentioned in scheme 1 i.e. benzylation, lithium hydroxide mediated de-esterification and amidation to afford the synthesis of target compounds (**8**, **10**, **12**, **14-16)**. The synthesis of the target compound **9** was accomplished as per the synthetic protocol shown in scheme 3. The starting material **19** (2,6-dichloro-9H-purine) underwent condensation with methyl 4-aminobenzoate catalyzed via mineral acid followed by ester hydrolysis and EDC/HOBt mediated amidation with NH_2OTHP employing N,N-Diisopropylethylamine as the base to yield intermediate **51**. Benzylation of the intermediate **51** at position 9 with methyl 4-(bromomethyl)benzoate and subsequent de-esterification gave the

carboxylic acid **53**. The acid **53** was treated with o-phenylene diamine to yield intermediate **54** which underwent TFA-mediated deprotection to afford the target compound **9**. Scheme 4 presents the synthetic route to benzamide **18**. Initially, numerous attempts (not shown in scheme 4) were made to incorporate the 2,4,6-trichloro-3,5-dimethoxy aniline functionality via N-methyl urea tetheration at position 4 of the 7H-pyrrolo[2,3-d]pyrimidin-2-ylamine core. However, the condensation was not successful and an alternative strategy was employed which led to the condensation of the desired aniline at position 2. The starting material **22** was treated with methyl amine to give intermediate **55** which was converted to isocyanate via treatment with triphosgene and then reacted with the desired aniline. The subsequent route to furnish target compound **18** was similar to that employed in previous schemes.

2.2. Biological evaluation

2.2.1 Antiproliferative activity

The synthesized compounds (**7**-**18**) were evaluated for *in vitro* cytotoxicity against the triple-negative breast cancer cells (MDA-MB-231) as this type of cancer have been found highly malignant and lack of efficient therapeutics and HDAC2 and 3 were highly expressed in breast tumors isolated from hormone receptor-negative patients [26]. Given HDAC1-3 were also found to be upregulated in clinical samples of human hepatocellular carcinomas (HCCs) [27], we also

tested the effects of our compounds on the viability of HepG2. MS-275 (**5**) and CFDA-approved Chidamide (**6**) were employed as internal standards and the results are depicted in Table 1. The study reveals exciting insights regarding the cytotoxic effects of the synthesized aminoanilides. In general, the cancer cell lines exhibited a similar trend of sensitivity to the exposure of the test compounds as that to MS-275 (**5**) and Chidamide (**6**) with MDA-MB-231 cell line being the more sensitive one. Careful observation of Table 1 clearly indicates the influence of amine group at position 2 on the cellular activity of the benzamides as replacement of the chloro group (**7, 11**) with amino group (**13**, **17**) induced cell growth inhibitory effects against both cell lines. Induction of cytotoxicity against MDA-MB-231 was also evidenced with the placement of 3-chloro-4-flouro aniline functionality at position 6 in compounds bearing the purine core with chloro substitution at position 2 (compare **7** and **8**). Similarly, fusion of the purine core with 4-methyl-1H-pyrazol-3-yl functionality induced cell growth inhibition towards the cell lines employed (compare **7** and **10**). However, the trend was not replicated with the corresponding compounds bearing the 7H-pyrrolo[2,3-d]pyrimidine core as isosteric CAP construct (compare **11** and **12**). Incorporation of 3-chloro-4-flouro aniline functionality (at position 6) emerged to be most effective for the purine based benzamides with amine group at position 2 (compare compound **13** and **14**). Compound **14** exhibited the most substantial effects against the cell lines employed with IC_{50} values of 1.48 ± 0.06 µM (MDA-MB-231) and 2.44 ± 0.18 µM (HepG2). It

was interesting to observe that the cell growth inhibitory potential of compound **14** was higher than MS-275 (**5**) and Chidamide (**6**). In light of these effects, we also observed consistent results from another TNBC cell line, MDA-MB-468, which showed higher sensitivity to **14** in comparison to MS-275 and Chidamide (Fig. 3). In contrast, the breast cancer cell line positive for estrogen and progesterone receptors MCF-7 was more resistant to these compounds and did not show higher susceptibility to **14** (Fig. 3). It is tempting to speculate that the expression of the receptors may contribute to the cytotoxicity of these benzamide derivatives in breast cancer cells. Further structural optimization studies involved the replacement of 3-chloro-4-flouro aniline with 3,5- dimethoxy aniline (compare **14** with **15**) at position 6 and N-(2-aminophenyl) functionality (zinc binding motif) with N-(2-amino-5-fluorophenyl) functionality (compare **17** with **13**). The replacement led to decrease in the cellular activity for compound **15**, however the placement of N-(2-amino-5-fluorophenyl) functionality as the zinc binding group (compound **17**) retained the activity against both the cell lines. Isosteric replacement of purines as CAP construct in benzamide **14** yielding the counterpart **16** also demonstrated a decline in cell growth inhibitory effects. Compound **18** with 2-(3-(2,4,6-trichloro-3,5-dimethoxyphenyl)ureido) moiety at position 2 was devoid of cell killing effects. In general, benzamides with purine scaffold as the CAP construct caused greater inhibition of the cell growth and also favored the inclusion of substituted anilines and amines at position 6. Overall, presence of amine group,

3-chloro-4-flouro aniline functionality and the CAP construct remarkably influenced the cytotoxic effects of the compounds.

2.2.2 HDAC isoform inhibition

All the compounds were tested for enzyme inhibitory activity towards the HDAC1, 2, 6 and 8 isoforms as shown in the Table 2. MS-275 (**5**) was employed as a reference compound in the study. Most of the benzamides were endowed with potent and selective inhibitory profile towards the HDAC1 and 2 isoforms. Among them, compound **9** possessing weak cell growth inhibitory effects (Table 1) stands as an exception displaying strikingly selective inhibitory potential against the HDAC6 isoform (IC_{50} = 11.3 nM). Apart from HDAC6, other isoforms were also significantly inhibited by compound **9** with IC_{50} values of 0.182 μM (HDAC1), 1.45 μM (HDAC2) and 0.352 μM (HDAC8). The selectivity towards the HDAC6 isoform could be attributed to the structural orientation of **9** possessing hydroxamic acid functionality. Overall, compound **9**, **10**, **13**, **14**, **15** and **16** displayed higher inhibition against the HDAC1 isoform in comparison to the standard, **5**. The most cytotoxic benzamide **14** inhibited the HDAC1 and 2 isoform with IC_{50} values of 0.108 μM and 0.585 μM. On the contrary, benzamide **15** which as such was less potent in inhibiting the growth of cell lines caused the most substantial HDAC1 and 2 isoform inhibition with IC_{50} values of 0.0239 μM (HDAC1) and 0.179 μM (HDAC2). A 15-fold higher selectivity was displayed by **15** towards the HDAC1 isoform in comparison to

HDAC2**.** Conclusively, both the benzamides (**14** and **15)** were more potent than MS-275 (**5**) against the HDAC1 as well as HDAC2 isoform. Another benzamide **16** with moderate inhibitory potential against the cancer cell lines displayed substantial selective inhibition towards HDAC1 over the HDAC2 isoform (639 folds, IC_{50} = 93 nM). Collectively, the results indicate that the isosteric replacement of purine core (benzamide **14**) with 7H-pyrrolo[2,3-d]pyrimidine furnishing benzamide **16** was found to be effective in potentiating the inhibition as well as selectivity towards the HDAC1 isoform. Unlike the cytotoxic profile, 3,5 –dimethoxy aniline ring (**15**) was found to be the most instrumental in inducing potent inhibitory effects towards the HDAC1 and 2 isoforms**.**

2.2.3 Evaluation of inhibitory effects of benzamide 14 towards all the HDAC isoforms

In view of the remarkable antiproliferative effects of benzamide **14** against the human cancer cell lines employed along with substantial inhibition of HDAC1 and 2 isoforms, the compound was further evaluated against all the HDAC isoforms and the results are depicted in Table 3. The results of evaluation indicate a more pronounced inhibition of HDAC1, 2 and 3 by **14** with IC_{50} values of 0.108, 0.585 and 0.563 μM in comparison to MS-275. Among these isoforms, benzamide **14** preferentially inhibited HDAC1 over HDAC2 and HDAC3 and was 5 folds more potent than the standard against the HDAC1 isoform. The results presented in Table 3 ascertain the potential of **14** as class I HDAC inhibitor.

2.2.4 *In vitro* cytotoxicity studies against HDAC inhibitors resistant and sensitive in gastric cancer cell lines

Cancers display variable sensitivity to HDAC inhibitors. Previous studies have identified a series of gastric cancer cell lines exhibiting differential response to HDAC inhibitors [28]. Consistent to this report, the YCC3/7 cells showed more resistant to MS-275 (**5**) in comparison to the sensitive cell line YCC11 (Table 4). The values of 50% growth inhibition concentration (IC_{50}) of MS-275 in YCC3/7 and YCC11 were 12.98 ± 1.02 μM and 6.03 ± 0.44 μM, respectively. Similar trend was also observed in the two cell lines treated with compounds **10**, **11**, **13** and **17**. In contrast, compounds **8**, **14**, **15**, **16** and Chidamide (**6**) showed non-differential toxicities to two cell lines. Among these, **14** was the most virulent in both cells lines, with IC_{50} values of 4.79 ± 0.37 μM and 4.77 ± 0.29 μM in YCC3/7 and YCC11 cells, respectively. Taken together, these results reveal **14** as a potent anti-cancer agent that can overcome HDACi resistance.

2.2.5 *In vitro* cytotoxicity studies against leukemic cell lines

To gain further insights into the application of compound **14**, we compared the potency of **14**, MS-275, Chidamide and SAHA against three leukemic cell lines that have been tested in previous studies [29-34]. We found that these compounds exhibited strong toxicities in all three tested leukemic cell lines, with IC_{50} values below micromolar (Fig. 4), lower than that of most of

the solid tumor cell lines we used in the study (Tables 1, 4 and Fig. 3). It's worth noting that the IC_{50} values of **14** in these cell lines were highly similar (~0.33 μM). All three leukemic cell lines showed significantly higher sensitivities to **14** than SAHA. In contrast, MS-275 and Chidamide did not possess higher activity than SAHA in K-562 cells. These differential sensitivities provide important information for selection of HDAC inhibitors in leukemia treatment.

2.2.6 Interaction analysis of compound 14 in HDAC1

To provide a proof of concept of our molecular docking protocol, we first re-docked the co-crystal ligand into its target protein active site similar to that performed in the literature [35, 36]. The docked ligand poses showed similar conformations with the co-crystal ligands of HDAC1 and HDAC2 (Supporting information, Fig. 1S). The structure of HDAC3 (PDB ID: 4A69) was not used for validation because the co-crystal ligand is not an HDAC inhibitor. Nevertheless, the results suggest that favorable accuracy is obtained with the docking protocol and methodology used in this study. For clarity, analysis of the docked compound is separated into three sections: Zinc binding group (ZBG), linker and cap group. These sections are observed with traditional HDAC inhibitor [37]. The ZBG of compound **14** contains a N-(2-aminophenyl)formamide moiety. Chelating the zinc ion is crucial for HDAC inhibition [38]. This is achieved with the carbonyl oxygen of benzamide **14** which also forms a hydrogen bond with residue Y303 (Fig. 5). The ZBG contains a primary amine and an amide NH. A

primary amine located on the aromatic ring forms hydrogen bonds to two residues, His140 and His141. The amide NH forms a hydrogen bond to residue Gly149 (Fig. 5). Both the amine and the amide NH function as hydrogen bond donors. Hydrophobic interactions with residues M30, L139, H140, H141 and G300 sandwich the aromatic ring of the ZBG. Together, these interactions, combined with zinc chelation, acts as an anchor for compound **14** in the HDAC1 active site. The benzyl moiety functions as the linker and spans a hydrophobic tunnel to connect the ZBG to the cap group [39]. The aromatic ring of benzyl functionality facilitates hydrophobic interactions with ring residues F150, H178 and F205 (Fig. 5). The cap group of compound **14** lies at the periphery of the HDAC1 active site. This group consists of a N6-(3-chloro-4-fluorophenyl)-9H-purine-2,6-diamine moiety. This moiety is bulky and contains multiple ring structures. We observed one hydrogen bond between the amine moiety and residue D99 (Fig. 5). The chlorine and fluorine halogens are positioned outside of the active site entrance. A hydrophobic interaction is present between residue L271 and the chlorine moiety. This allows the cap to occupy a pocket without steric clashes along the HDAC1 active site. Together, we found that compound **14** can form favorable interactions within the HDAC1 active site.

2.2.7 Binding interactions of compound 14 in HDAC isozymes

Next, we sought to compare the interactions of compound **14** in HDAC isozymes. The HDAC isozymes are typically separated into four families: Class I, IIa, IIb, and IV [38]. Compound **14** was found to have the greatest inhibitory effect on HDAC1 (Class I) (Table 2). When docked into HDAC4 (Class IIa), the position of compound **14** is flipped with respect to its pose in HDAC1 (Fig. 6A). This is attributed to differences with two amino acids in the active site. First, the ring structure of residue Y303 is pointed into the active site in HDAC1, while the ring structure of residue H976 in HDAC4 is pointed away. This residue change in HDAC4 removes a hydrogen bond in the active site, compared to the interaction formed between compound **14** and residue Y303 in HDAC1. Furthermore, the ring structure of residue P800 of HDAC4 reduces a pocket within the active site. As a result, compound **14** does not have favorable binding to HDAC4.

Compound **14** also shows poor inhibition of HDAC6 (Table 2). The carbonyl oxygen, which functions as the chelator in HDAC1, is not in a favorable distance to chelate the HDAC6 zinc ion (Fig. 6B). When the docking results were superimposed, we observed that compound **14** does not penetrate the HDAC6 active site as deep as that seen in HDAC1. This may be due to HDAC6 residue P608, which creates a shallower pocket due to its ring pointing towards the active site, compared to residue L139 found in HDAC1. Furthermore, HDAC6 residue S568 does not form a hydrogen bond with the cap group, which may reduce the potency of the compound (Fig. 6B).

HDAC1 and HDAC8 are both grouped as class I HDACs. However, compound **14** produces a significantly higher inhibition of HDAC1 isoform (Table 2). Compared to HDAC4 and HDAC6, the pose of compound **14** in HDAC8 is closer to the one observed in HDAC1 (Fig. 5C). This can be attributed to the class similarity of HDAC1 and HDAC8. However, two differences were observed that may account for the weaker inhibition of the compound. The cap forms a hydrogen bond with HDAC1 residue D99. In HDAC8, the cap is rotated away from the respective residue, D101. This may also force the compound **14** cap to occupy a different position in the periphery of the HDAC active site. In addition, HDAC8 contains residue M274 instead of residue L271 found in HDAC1. As a result, HDAC8 lacks a hydrophobic interaction with the CAP construct of compound **14** at this position. Together, these interactions show the preference of compound **14** towards HDAC1.

Overall, the docking results supports the substantial HDAC1 inhibition exerted by benzamide **14** in comparison to the other HDAC isozymes. Some key interactions with the amino acid residues of HDAC1 isoform were figured out to rationalize the experimental findings such as i) ZBG of compound **14** chelates the HDAC1 zinc ion and forms hydrogen bonds to residues H140, H141 and G149. (Fig. 5) ii) The linker of compound **14** consists of a benzyl moiety that spans the HDAC1 hydrophobic tunnel. iii) Cap construct of **14** forms hydrophobic interactions with residue L271 and a hydrogen bond to residue D99 (Fig. 5). Overall, the interactions along the

rim of the active site may explain a greater inhibitory activity of compound **14** towards HDAC1 isoforms. Moreover, these results are in resonance with the results of studies revealing key insights regarding the catalytic domains of HDAC isoforms [40-43] and suggests the importance of the cap group in determining HDAC selectivity. Together, these interactions rationalize the selectivity of compounds **14** towards HDAC1.

We also docked compound **14** into HDAC2 and HDAC3 to determine its binding interactions. Overall, we observed similar binding poses of Compound **14** in HDAC1-3 (Fig. 5). Importantly, the ZBG coordinated to the metal zinc ion and no steric hindrance of the linker group was observed. These poses suggest Compound **14** has inhibitory activity towards HDAC1, HDAC2 and HDAC3.

Next, we performed a molecular dynamics (MD) simulation to determine important residues for binding interactions between the ligand and HDAC1 protein structure. The final conformation of the Compound **14**-HDAC1 complex was similar to its docked pose (Fig. 7A-B). Important interacting residues from the MD simulation were identified (Fig. 7C). The metal coordination is key for HDAC inhibition and was observed throughout the MD simulation. Hydrogen bonds occur with greater frequency with residues D99 and D176. Prominent hydrophobic interactions were observed with residues M30, C151, Y204, F205, L271 and C273. Many of these hydrophobic interactions occur with the hydrophobic tunnel and the compound **14**

linker, however, hydrophobic interactions occur between residues L271 and C273 and the cap group. A halogen interaction between the cap group and residue C273 also occurred with greater frequency. Together, the MD simulation suggests that compound **14** binds effectively to the HDAC1 active site.

2.2.8 HDAC inhibitory activity in human breast cancer cell line.

Histones are wildly used substrates to determine the activity of most HDACs *in vitro*. However, only HDAC1, 2 and 3, as well as Sir2-like enzymes, have been validated to deacetylate histones in cells [44-45]. In contrast, the main targets of other HDACs *in vivo* are non-histone proteins, such as α-tubulin for HDAC6 and structural maintenance of chromosomes protein 3 (SMC3) for HDAC8 [46-47]. Compound **14** and **16** were thus further selected for the Western blot analysis to ascertain their ability to modulate the protein levels of important biomarkers associated with intracellular HDAC inhibition. This could help establish the effects of subtle structural variation (purine and its isosteric scaffold) in the surface recognition part on the HDAC inhibition. We determined the acetylation levels of different HDAC substrates in MDA-MB-231 cells and exploited Tubastatin A and PCI-34051 as controls for suppression of HDAC6 and HDAC8i, respectively. (Fig. 8). Similar to the effect of MS-275, we observed a dose-dependent upregulation of the acetylation levels on the 9th lysine of histone H3 (ac-H3 K9) and the $5/8/12/16^{th}$ lysine of histone H4 (ac-H4 K5/8/12/16) in cells treated with the compound

14 and **16**. In contrast, the level of aectylated α-tubulin and SMC3 were not affected (Fig. 8A). These results were consist with *in vitro* HDAC inhibition study and molecular docking analysis, supporting that benzamide 14 behaves as a class I HDAC inhibitor targeting to HDAC1, 2 and 3.

2.2.9 G_1 phase arrest and apoptosis in human breast cancer cell line.

The data present in this study indicate that the benzamide derivative **14** possesses strongly inhibitory activity against HDAC1, 2 and 3 (Table 2 and 3). HDACs are known to control cell proliferation through regulation of cell cycle progression, apoptosis and other cellular activities [48]. Consistent to the previous studies [32, 49, 50], our Western blot analysis showed that HDAC inhibition by **14**, **16** or MS-275 increased the expression of the cyclin-dependent kinase (CDK) inhibitor p21 (Fig. 8A) in a dose-dependent manner, perhaps through suppressing HDAC1 and 2 bound on p21 promoter [51, 52]. Given that excess expression of p21 can disturb cell cycle progression and MS-275 has been known to elicit p53-dependent cell death [53, 54], we further determined the cell status of cells treated with these compounds to establish the influence of amino group as well as isosteric replacement of the purine core.

To this, we treated MDA-MB-231 cells with a low dose (4 μM) of the standard compound (**5**) and the benzamides (**14** and **16**) for 24 hours, followed by analysis of cell cycle distribution with flow cytometry. Cells treated with individual compound exhibited a cell cycle profile similar to control but lost the population of S phase, the stage between G_1 to G_2/M phases (Fig. 9A),

suggesting that those cells are unable to initiate DNA replication. We further evaluated the efficiency of cell cycle progression by measuring the rate of accumulation of mitotic cells in the presence of nocodazole, an inhibitor of microtubule polymerization. Compared to the control cells that accumulated in G2/M after nocodazole treatment, a large portion of cells treated with tested compounds stayed in G_1 (Fig. 9A). These results clearly demonstrate that the benzamide **14** and **16** function as HDAC1 inhibitors that are able to trigger cell cycle arrest in G_1.

As expected, the higher dose (16 μM) of MS-275 induced cell death detected by accumulation of subG_1 population at 48 hours after treatment (Fig. 9B). This effect was more pronounced when cells were treated with **14** (Fig. 9B). We thus further investigated their efficiency of apoptosis induction by measuring the level of cleavage of caspases and PARP-1, indicatives of apoptosis activation. Our results from Western blot analysis showed that cleaved forms of caspase-3, -8 and PARP-1 were significantly increased in MDA-MB-231 cells treated with the test compounds (Fig. 9C). Notably, benzamide **14** was endowed with more potent effect in subG_1 accumulation and activation of apoptotic pathway, as compared to **5** and **16** (Fig. 9B-C). These results highlight the apoptosis inducing ability of the selected benzamides with most substantial effects displayed by benzamide **14**, consistent with the growth suppression observed (Table 1). The outcome of the assay also indicates the favorable effects attained via placement of amine group on the purine core linked to 3-chloro-4-floro aniline functionality.

2.2.10 Antitumor efficacy of compound 14 in human MDA-MB-231 breast cancer xenograft model

Compound **14** was evaluated for *in vivo* efficacy against tumor xenografts in human MDA-MB-231 breast cancer cells. The tumor growth curve and animal body weight change for each treatment group are shown in Fig. 10. As shown in Fig. 10A, Taxol at 10 mg/kg (intravenous injection, every other day) ($p<0.05$) and compound **14** at 50 mg/kg (intraperitoneal injection, every day) ($p<0.01$) produced significant antitumor activity and suppressed the growth of MDA-MB-231 breast cancer xenografts by tumor growth inhibition values (TGI) of 32.5% and 56.3%, respectively. Moreover, there were no significant changes in body weight at all doses tested (Fig. 10B). Overall, the result demonstrates that compound **14** is endowed with potent *in vivo* antitumor efficacy in human MDA-MB-231 breast cancer xenograft model.

3. Conclusion

This study dealt with the structural optimization of MS-275 (**5**) and Chidamide (**6**) to furnish more potent antiproliferative agents. Specifically, attempts were made towards the inclusion of purine/purine isoster as a bicyclic heteroaryl CAP construct and the replacement of carbamate and acrylamide group as a connecting unit to the linker in the design of class I HDAC inhibitors.

The approach was further extended to link the CAP constructs with substituted anilines and appropriate amines reported to exert anticancer effects. The results of the *in-vitro* assays led us generate structure-cytotoxicity as well as structure-HDAC isoform inhibition relationship which in turn established the impact of variations in the CAP component on the bioactivity (Fig. 11). It was observed that the placement of substituted aniline at position 4 was favored for antiproliferative effects as well as significant Class I HDAC inhibition. Specifically, 3-chloro-4-fluoroaniline was found to be the preferred substitution for cell growth inhibitory effects and for class I HDAC inhibition, 3,5-dimethoxyaniline was the substituent of choice. Other than this, factors such as utilization of the purine core in the design of the target constructs and the presence of amine group at position 2 were identified to be instrumental for inducing the antiproliferative effects (Fig. 11). The structural notions generated in this study provides us valuable information that can be further utilized for the extension of our research work centered at the design of purine/purine isoster based HDAC inhibitor. Subsequently, the results of biological evaluation led us identify a potent class I HDAC inhibitor **14** which was found to be the most virulent in HDACi resistant (YCC3/7) as well as sensitive (YCC11) gastric cell lines. These are optimistic findings as they are indicative of the capacity of benzamide **14** to overcome HDACi resistance in gastric cancer which is the one of the most common cause of cancer-related deaths and fabrication of treatment strategies via design of small molecule inhibitors is the need

of the hour. To add on, the *in vitro* cytotoxicity studies demonstrating the efficacy of benzamide **14** against the triple negative breast cancer cell line (TNBC, MDA-MB-231 and MDA-MB-468) is an equally important finding in view of the lack of biomarkers for their targeted therapy. As such, TNBC demonstrates lack of sensitivity towards the existing systemic therapies and have also been evidenced to incur a high rate of recurrence [55]. In this context, the revelations of this study are significantly promising. Moreover, HDAC inhibitor **14** exhibited significant inhibitory potential against K-562, THP-1, KG-1 and HL-60 cancer cell lines, exerted a dose-dependent upregulation of ac-H3K9 in MDA-MB-231 cells and also triggered cell cycle arrest in G1 phase. The results of the docking study highlight the importance of the cap group in determining HDAC selectivity and identified key interactions that forms the basis of compounds **14'**s selectivity towards HDAC1. Furthermore, benzamide **14** also demonstrated potent *in vivo* antitumor efficacy in human MDA-MB-231 breast cancer xenograft model. These evidences and the lack of clinically approved benzamides with the exception of Chidamide (**6**) as the only benzamide type HDAC inhibitor clearly ascertains the need of detailed investigation of benzamide **14.** In a nut shell, compound **14** could emerge as a potential lead compound for the development of anti-breast and gastric cancer agent. Further lead modifications on **14** such as synthesis of compounds with diverse substitutions on the purine and its isoster core along with utilization of other linkers is under progress.

4. Experimental

4.1. Chemistry

Nuclear magnetic resonance spectra were obtained with Bruker DRX-500 spectrometer (operating at 300 MHz), with chemical shift in parts per million (ppm, d) downfield from TMS as an internal standard. High-resolution mass spectra (HRMS) were measured with a JEOL (JMS-700) electron impact (EI) mass spectrometer. Purity of the final compounds were determined using an Hitachi 2000 series HPLC system using C-18 column (Agilent ZORBAX Eclipse XDB-C18 5 mm. 4.6mm_ 150 mm) and were found to be > 95%. Flash column chromatography was done using silica gel (Merck Kieselgel 60, No. 9385, 230e400 mesh ASTM). All reactions were carried out under an atmosphere of dry nitrogen.

4.1.1 Synthesis of methyl 4-((2,6-dichloro-9H-purin-9-yl) methyl) benzoate (23)

A mixture of 4-chloro-7H-pyrrolo[2,3-d] pyrimidin-2-amine (**19**) (0.5 g, 2.64 mmol), methyl 4-(bromomethyl) benzoate (0.605 mg, 2.64 mmol) and potassium carbonate (0.547 mg, 3.96 mmol) in DMF was stirred at 60 °C for 4h. The reaction mixture was quenched with H_2O and extracted with EtOAc (50 mL x 3). The combined organic layer was dried over anhydrous $MgSO_4$, concentrated under reduced pressure and purified by silica gel chromatography to give

compound **23** in 73 % yield; ^{1}H NMR (300 MHz, CD_3OD): 8.21 (s, 1H), 7.89 (d, J = 8.7 Hz, 2H), 7.49 (d, J = 8.7 Hz, 2H), 5.21 (s, 2H), 3.81 (s, 3H).

Synthesis of methyl 4-((2,4-dichloro-7H-pyrrolo[2,3-d] pyrimidin-7-yl)methyl) benzoate (24)

The title compound **24** was synthesized from compound 2,4-Dichloro-7H-pyrrolo[2,3-d]pyrimidine **(20)** in a manner similar to that described for the synthesis of compound **23**; ^{1}H NMR (300 MHz, CD_3OD): 7.89 (d, J = 8.1 Hz, 2H), 7.28 (d, J = 8.1 Hz, 2H), 7.08 (d, J = 3.9 Hz, 1H), 6.31 (d, J = 3.9 Hz, 1H), 5.23 (s, 2H), 3.79 (s, 3H).

Synthesis of methyl 4-((2-amino-6-chloro-9H-purin-9-yl) methyl) benzoate (25)

The title compound **25** was synthesized from compound 6-chloro-9H-purin-2-amine (**21)** in a manner similar to that described for the synthesis of compound **23**; ^{1}H NMR (300 MHz, CD_3OD): 8.21 (s, 1H), 7.76 (d, J = 8.7 Hz, 2H), 7.46 (d, J = 8.7 Hz, 2H), 5.35 (s, 2H), 3.79 (s, 3H).

Synthesis of methyl 4-((2-amino-4-chloro-7H-pyrrolo[2,3-d] pyrimidin-7-yl) methyl) benzoate (26)

The title compound **26** was synthesized from 4-chloro-7H-pyrrolo[2,3-d] pyrimidin-2-amine (**22)** in a manner similar to that described for the synthesis of compound **23**; ^{1}H NMR (300 MHz,

CD_3OD): 7.85 (d, J = 8.0 Hz, 2H), 7.21 (d, J = 8.0 Hz, 2H), 7.14 (d, J = 3.5 Hz, 1H), 6.28 (d, J = 3.5 Hz, 1H), 5.24 (s, 2H), 3.81 (s, 3H).

Synthesis of 4-((2,6-dichloro-9H-purin-9-yl) methyl) benzoic acid (27)

A mixture of compound **23** (0.6 g, 1.77 mmol), 1M LiOH aq. (10 ml) and dioxane (20 mL) was stirred at room temperature for 2 h. The reaction was concentrated under reduced pressure and H_2O was added. The mixture was acidified with 3N HCl and extracted with EtOAc (50 mL x 3). The combined organic layer was dried over anhydrous $MgSO_4$ and concentrated under reduced pressure to yield the acid (**27**) in 96% yield; ^{1}H NMR (300 MHz, CD_3OD): 8.29 (s, 1H), 7.92 (d, J = 8.1 Hz, 2H), 7.57 (d, J = 8.1 Hz, 2H), 5.34 (s, 2H).

Synthesis of 4-((2,4-dichloro-7H-pyrrolo[2,3-d] pyrimidin-7-yl) methyl) benzoic acid (28)

The title compound **28** was synthesized in 97 % yield from compound **24** in a manner similar to that described for the synthesis of compound **27**. ^{1}H NMR (300 MHz, CD_3OD): 7.98 (d, J = 8.1 Hz, 2H), 7.29 (d, J = 8.1 Hz, 2H), 7.06 (d, J = 3.9 Hz, 1H), 6.39 (d, J = 3.9 Hz, 1H), 5.29 (s, 2H).

Synthesis of 4-((2-amino-6-chloro-9H-purin-9-yl) methyl) benzoic acid (29)

The title compound **29** was synthesized in 94 % yield from compound **25** in a manner similar to that described for the synthesis of compound **27**. ^{1}H NMR (300 MHz, CD_3OD): 8.27 (s, 1H), 7.89 (d, J = 8.7 Hz, 2H), 7.41 (d, J = 8.7 Hz, 2H), 5.33 (s, 2H).

Synthesis of 4-((2-amino-4-chloro-7H-pyrrolo[2,3-d] pyrimidin-7-yl) methyl) benzoic acid (30)

The title compound **30** was synthesized in 96 % yield from compound **26** in a manner similar to that described for the synthesis of compound **27**. ^{1}H NMR (300 MHz, CD_3OD): 7.98 (d, J = 8.0 Hz, 2H), 7.43 (d, J = 8.0 Hz, 2H), 7.14 (bs, 1H), 6.39 (d, J = 3.5 Hz, 1H), 5.23 (s, 2H).

Synthesis of N-(2-aminophenyl)-4-((2,6-dichloro-9H-purin-9-yl) methyl) benzamide (7)

A mixture of compound **27** (0.5 g, 1.54 mmol), EDC.HCl (0.591 g, 3.09 mmol), HOBt (0.311 g, 2.31 mmol), benzene-1,2-diamine (0.166 g, 1.54 mmol) and DIPEA (0.718 ml, 4.13 mmol) in DMF (5 mL) was stirred at RT for 5 h. After being stirred for a further 5 h, the reaction mixture was quenched with H_2O and extracted with EtOAc (50 mL x 3). The combined organic layer was dried over anhydrous $MgSO_4$, concentrated under reduced pressure and purified by silica gel chromatography (hexane: EtOAc = 1:1) to give **7** in 71 % yield; mp: 180 -182 °C; ^{1}H NMR (500 MHz, CD_3OD): 8.15 (s, 1H), 7.95 (d, J = 8.5 Hz, 2H), 7.45 (d, J = 8.0 Hz, 2H), 7.17 (d, J = 7.0 Hz, 1H), 7.05 (m, 1H), 6.89 (d, J = 8.5 Hz, 1H), 6.76 (t, J = 8.5 Hz, 1H), 5.42 (s, 2H). ^{13}C (125 MHz, DMSO-d_6): 164.90, 159.91, 159.36, 158.76, 156.61, 154.05 149.52, 143.18, 143.04, 139.88, 134.11, 128.11, 127.05, 126.62, 123. 28, 119.86, 116.06, 109.39, 45.88. HRMS (ESI) for $C_{19}H_{15}Cl_2N_6O$ ($M+H^+$): calcd, 413.0684; found, 413.0928; LRMS - MS (ESI): 413.05 [M+H], 411.05 [M-H].

Synthesis of N-(2-aminophenyl)-4-((2,4-dichloro-7H-pyrrolo[2,3-d] pyrimidin-7-yl) methyl) benzamide (11)

The title compound **11** was synthesized in 75 % yield using compound **28** in a manner similar to that described for the synthesis of compound **7**; mp: 190 -191 °C; ^{1}H NMR (500 MHz, CD_3OD): 7.81 (d, J = 8.0 Hz, 2H), 7.22 (d, J = 8.0 Hz, 2H), 7.18 (d, J = 3.5 Hz, 1H), 7.14 (d, J = 7.5 Hz, 1H), 6.91 (m, 1H), 6.71 (d, J = 8.0 Hz, 1H), 6.51 (t, J = 7.5 Hz, 1H), 6.37 (d, J = 3.5 Hz, 1H), 5.31 (s, 2H). ^{13}C (75 MHz, DMSO-d_6): 165.50, 159.97, 154.05, 151.82, 143.57, 142.05, 141.52, 134.35, 133.85, 131.70, 128.37, 127.33, 126.94, 123.69, 116.71, 116.56, 109.09, 99.53, 47.34. HRMS (ESI) for $C_{20}H_{16}Cl_2N_5O$ ($M+H^+$): calcd, 412.0932; found, 412.0963.

Synthesis of 4-((2-amino-6-chloro-9H-purin-9-yl) methyl)-N-(2-aminophenyl) benzamide (13)

The title compound **13** was synthesized in 74 % yield using compound **29** in a manner similar to that described for the synthesis of compound **7**; mp: 194 -195 °C; ^{1}H NMR (500 MHz, CD_3OD): 8.19 (s, 1H), 8.09 (d, J = 8.7 Hz, 1H), 7.88 (d, J = 8.1 Hz, 2H), 7.65 – 7.66 (m, 2H), 7.55 (m, 1H), 7.46 (d, J = 8.4 Hz, 2H), 5.47 (s, 2H). ^{13}C (125 MHz, CD_3OD): 167.99, 161.89, 158.12, 151.73, 144.71, 144.59, 141.63, 135.72, 129.64, 128.99, 127.99, 126.60, 119.22, 118.49, 110.65, 48.72. HRMS (ESI) for $C_{19}H_{16}ClN_7O$ ($M+H^+$): calcd, 394.1183.; found, 394.1183.

Synthesis of 4-((2-amino-4-chloro-7H-pyrrolo[2,3-d] pyrimidin-7-yl) methyl) -N-(2-amino-5-fluorophenyl) benzamide (17)

The title compound **17** was synthesized in 12 % yield via two steps starting with the formation of amide using compound **30** and 4-fluorobenzene-1,2-diamine in a manner similar to that described for the synthesis of compound **7** followed by the deprotection of the *tert*-butyloxycarbonyl protecting group by trifloroacetic acid; mp: 240 - 242 °C; ^{1}H NMR (300 MHz, DMSO-d_6): 9.55 (s, 1H), 7.93 (d, J = 8.1 Hz, 2H), 7.29 (d, J = 8.4 Hz, 2H), 7.26 (d, J = 3.6 Hz, 1H), 7.11 (m, 1H), 6.71 (s, 2H), 6.55 (dd, J = 3.0 and 11.1 Hz, 1H), 6.38 (d, J = 3.3 Hz, 1H), 6.34 (t, J = 3.0 and 8.4 Hz, 1H), 5.35 (s, 2H), 5.23 (s, 2H). ^{13}C (125 MHz, CD_3OD): 165.21, 161.77, 160.19, 159.43, 153.53, 145.39, 140.99, 133.71, 128.46, 128.05, 126.79, 126.39, 119.12, 108.57, 102.03, 101.88, 101.29, 98.99, 46.81. HRMS (ESI) for $C_{19}H_{15}ClFN_7O$ ($M+H^+$): calcd, 411.1136; found, 411.1138.

Synthesis of 2-chloro-N-(3-chloro-4-fluorophenyl)-9H-purin-6-amine (31)

To the solution of compound **19** (1g, 5.29 mmol) in isopropanol (5 mL), 3-chloro-4-fluoroaniline (0.770 g, 5.29 mmol) and conc. HCl (0.5 mL) was added. The reaction mixture was refluxed for 5 h and water was added to it. Extraction was done with ethyl acetate (50 mL x 3). The combined organic layer was dried over anhydrous $MgSO_4$ and concentrated under reduced pressure. The resulting residue was purified by silica gel chromatography (n-hexane: EtOAc = 1 : 1) to give

compound **31** in 62 % yield; ^{1}H NMR (300 MHz, CD_3OD): 8.41 (s, 1H), 8.18 (m, 1H), 7.41 (m, 1H), 7.12 (d, J = 7.5 Hz, 1H).

Synthesis of 2-chloro-N-(4-methyl-1H-pyrazol-3-yl)-9H-purin-6-amine (32)

The title compound **32** was synthesized in 46 % yield using compound **19** and 4-methyl-1H-pyrazol-3-amine in a manner similar to that described for the synthesis of compound **31**. ^{1}H NMR (300 MHz, CD_3OD): 8.32 (s, 1H), 6.31 (s, 1H), 2.29 (s, 3H).

Synthesis of 2-chloro-N-(3-chloro-4-fluorophenyl)-7H-pyrrolo[2,3-d] pyrimidin-4-amine (33)

The title compound **33** was synthesized in 61 % yield using compound **20** in a manner similar to that described for the synthesis of compound **31**. ^{1}H NMR (300 MHz, CD_3OD): 8.11 (d, J = 6.9 Hz, 1H), 7.75 (m, 1H), 7.43-7.45 (m, 2H), 6.86 (d, J = 3.3 Hz, 1H).

Synthesis of N6-(3-chloro-4-fluorophenyl)-9H-purine-2,6-diamine (34)

The title compound **34** was synthesized in 51 % yield using compound **21** in a manner similar to that described for the synthesis of compound **31**. ^{1}H NMR (300 MHz, CD_3OD): 8.24 (m, 1H), 8.13 (s, 1H), 7.22 – 7.33 (m, 2H).

Synthesis of N6-(3,5-dimethoxyphenyl)-9H-purine-2,6-diamine (35)

The title compound **35** was synthesized in 56 % yield using compound **21** and 3, 5 dimethoxy aniline in a manner similar to that described for the synthesis of compound **31**. ^{1}H NMR (300 MHz, CD_3OD): 7.92 (s, 1H), 7.24 (d, J = 1.5 Hz, 2H), 6.65 (d, J = 8.7 Hz, 1H), 3.79 (s, 6H).

Synthesis of N4-(3-chloro-4-fluorophenyl)-7H-pyrrolo[2,3-d] pyrimidine -2,4-diamine (36)

The title compound **36** was synthesized in 77 % yield using compound **22** in a manner similar to that described for the synthesis of compound **31**. ^{1}H NMR (300 MHz, CD_3OD): 8.24 (d, J = 6.6 Hz, 1H), 7.93 (bs, 1H), 7.29 -7.33 (m, 2H), 6.56 (d, J = 3.9 Hz, 1H).

Synthesis of methyl 4-((2-chloro-6-((3-chloro-4-fluorophenyl)amino)-9H-purin-9-yl) methyl)benzoate (37)

The title compound **37** was synthesized in 73 % yield using compound **31** and methyl 4-(bromomethyl) benzoate in a manner similar to that described for the synthesis of compound **23**. ^{1}H NMR (300 MHz, CD_3OD): 8.41 (s, 1H), 8.18 (m, 1H), 7.87 (d, J = 8.1 Hz, 2H), 7.41-7.44 (m, 3H), 7.12 (d, J = 7.5 Hz, 1H), 5.39 (s, 2H), 3.86 (s, 3H).

Synthesis of methyl 4-((2-amino-6-((4-methyl-1H-pyrazol-3-yl)amino)-9H-purin-9-yl)methyl)benzoate (38)

The title compound **38** was synthesized in 75 % yield using compound **32** and methyl 4-(bromomethyl)benzoate in an manner similar to that described for the synthesis of compound

23. ^{1}H NMR (300 MHz, CD_3OD): 8.45 (s, 1H), 7.87 (d, J = 8.7 Hz, 2H), 7.49 (d, J = 8.7 Hz, 2H), 6.36 (s, 1H), 5.45 (s, 2H), 3.79 (s, 3H), 2.29 (s, 3H).

Synthesis of methyl 4-((2-chloro-4-((3-chloro-4-fluorophenyl)amino)-7H-pyrrolo[2,3-d]pyrimidin-7-yl)methyl)benzoate (39)

The title compound **39** was synthesized in 78 % yield using compound **33** and methyl 4-(bromomethyl) benzoate in a manner similar to that described for the synthesis of compound **23**. ^{1}H NMR (300 MHz, CD_3OD): 8.11 (d, J = 6.9 Hz, 1H), 7.75 – 7.92 (m, 4H), 7.43 – 7.49 (m, 3H), 6.86 (d, J = 3.3 Hz, 1H), 5.46 (s, 2H), 3.87 (s, 3H).

Synthesis of methyl 4-((2-amino-6-((3-chloro-4-fluorophenyl) amino)-9H-purin-9-yl) methyl) benzoate (40)

The title compound **40** was synthesized in 71 % yield using compound **34** and methyl 4-(bromomethyl) benzoate in a manner similar to that described for the synthesis of compound **23**. ^{1}H NMR (300 MHz, CD_3OD): 8.24 (m, 1H), 7.98 – 8.13 (m, 4H), 7.22 – 7.33 (m, 3H), 5.32 (s, 2H), 3.78 (s, 3H).

Synthesis of methyl 4-((2-amino-6-((3,5-dimethoxyphenyl)amino)-9H-purin-9-yl)methyl)benzoate (41)

The title compound **41** was synthesized in 78 % yield using compound **35** and methyl 4-(bromomethyl) benzoate in a manner similar to that described for the synthesis of compound **23**. ^{1}H NMR (300 MHz, CD_3OD): 7.92 (s, 1H), 7.83 (d, J = 8.7 Hz, 2H), 7.26 (d, J = 8.1 Hz, 2H), 7.24 (d, J = 1.5 Hz, 2H), 6.65 (d, J = 8.7 Hz, 1H), 5.35 (s, 2H), 3.73 (s, 6H).

Synthesis of methyl 4-((2-amino-4-((3-chloro-4-fluorophenyl)amino)-7H-pyrrolo[2,3-d] pyrimidin-7-yl)methyl)benzoate (42)

The title compound **42** was synthesized in 76 % yield using compound **36** and methyl 4-(bromomethyl) benzoate in a manner similar to that described for the synthesis of compound **23**. ^{1}H NMR (300 MHz, CD_3OD): 8.21 (d, J = 6.6 Hz, 1H), 7.91 – 7.97 (m, 3H), 7.48 (d, J = 7.2 Hz, 2H), 7.33 (m, 1H), 7.17 (m, 1H), 6.56 (d, J = 3.9 Hz, 1H), 4.87 (s, 2H), 3.83 (s, 3H).

Synthesis of 4-((2-chloro-6-((3-chloro-4-fluorophenyl)amino)-9H-purin-9-yl)methyl)benzoic acid (43)

The title compound **43** was synthesized in 97 % yield using compound **37** in a manner similar to that described for the synthesis of compound **27**. ^{1}H NMR (300 MHz, CD_3OD): 8.35 (s, 1H), 8.11 (m, 1H), 7.81 (d, J = 8.1 Hz, 2H), 7.51-7.53 (m, 3H), 7.16 (d, J = 7.5 Hz, 1H), 5.39 (s, 2H).

Synthesis of 4-((2-amino-6-((4-methyl-1H-pyrazol-3-yl)amino)-9H-purin-9-yl)methyl)benzoic acid (44)

The title compound **44** was synthesized in 93 % yield using compound **38** in a manner similar to that described for the synthesis of compound **27**. ^{1}H NMR (300 MHz, CD_3OD): 8.41 (s, 1H), 7.82 (d, J = 8.7 Hz, 2H), 7.41 (d, J = 8.7 Hz, 2H), 6.32 (s, 1H), 5.41 (s, 2H), 2.21 (s, 3H).

Synthesis of 4-((2-chloro-4-((3-chloro-4-fluorophenyl)amino)-7H-pyrrolo[2,3-d]pyrimidin-7-yl)methyl)benzoic acid (45)

The title compound **45** was synthesized in 91 % yield using compound **39** in a manner similar to that described for the synthesis of compound **27**. ^{1}H NMR (300 MHz, CD_3OD): 8.19 (d, J = 6.9 Hz, 1H), 7.65 – 7.87 (m, 4H), 7.41 – 7.43 (m, 3H), 6.81 (d, J = 3.3 Hz, 1H), 5.41 (s, 2H).

Synthesis of 4-((2-amino-6-((3-chloro-4-fluorophenyl)amino)-9H-purin-9-yl)methyl)benzoic acid (46)

The title compound **46** was synthesized in 95 % yield using compound **40** in a manner similar to that described for the synthesis of compound **27**. ^{1}H NMR (300 MHz, CD_3OD): 8.28 (m, 1H), 7.92 – 8.06 (m, 4H), 7.25 – 7.31 (m, 3H), 5.39 (s, 2H).

Synthesis of 4-((2-amino-6-((3,5-dimethoxyphenyl)amino)-9H-purin-9-yl)methyl)benzoic acid (47)

The title compound **47** was synthesized in 95 % yield using compound **41** in a manner similar to that described for the synthesis of compound **27**. ^{1}H NMR (300 MHz, CD_3OD): 8.02 (s, 1H),

7.88 (d, J = 8.7 Hz, 2H), 7.29 (d, J = 8.7 Hz, 2H), 7.21 (d, J = 1.5 Hz, 2H), 6.61 (d, J = 8.1 Hz, 1H), 5.28 (s, 2H).

Synthesis of 4-((2-amino-4-((3-chloro-4-fluorophenyl)amino)-7H-pyrrolo[2,3-d]pyrimidin-7-yl)methyl)benzoic acid (48)

The title compound **48** was synthesized in 95 % yield using compound **42** in a manner similar to that described for the synthesis of compound **27**. ^{1}H NMR (300 MHz, CD_3OD): 8.29 (d, J = 8.1 Hz, 1H), 7.87 – 7.92 (m, 3H), 7.42 (d, J = 7.2 Hz, 2H), 7.21 (m, 1H), 7.17 (m, 1H), 6.36 (d, J = 3.9 Hz, 1H), 4.98 (s, 2H).

Synthesis of N-(2-aminophenyl)-4-((2-chloro-6-((3-chloro-4-fluorophenyl)amino)-9H-purin-9-yl)methyl) benzamide (8)

The title compound **8** was synthesized in 65 % yield from compound **43** using benzene-1,2-diamine in a manner similar to that described for the synthesis of compound **7**. mp: 224 -225 °C; ^{1}H NMR (300 MHz, DMSO-d_6) : 10.57 (s, 1H), 9.64 (s, 1H), 8.53 (s, 1H), 8.14 (dd, J = 2.4 and 6.6 Hz, 1H), 7.98 (d, J = 8.1 Hz, 2H), 7.85 (m, 1H), 7.43-7.49 (m, 3H), 7.17 (d, J = 7.5 Hz, 1H), 6.96 (t, J = 7.5 Hz, 1H), 6.79 (d, J = 1.5 Hz, 1H), 6.60 (m, 1H), 5.53 (s, 2H), 4.90 (s, 2H). ^{13}C (125 MHz, DMSO-d_6): 164.88, 154.09, 152.48, 152.32, 152.12, 150.90, 143.06,

142.70, 139.56, 136.09, 134.24, 128.23, 127.24, 126.47, 123.14, 122.51, 121.43, 121.38, 118.82, 116.57, 116.18, 46.24. HRMS (ESI) for $C_{25}H_{18}Cl_2FN_7O$ (M+H+): calcd, 522.1012; found, 522.1009.

Synthesis of N-(2-aminophenyl)-4-((2-chloro-6-((4-methyl-1H-pyrazol-3-yl)amino)-9H-purin-9-yl)methyl)benzamide (10)

The title compound **10** was synthesized in 63 % yield from compound **44** using benzene-1,2-diamine in a manner similar to that described for the synthesis of compound **7**. mp: 171 -172 °C; ^{1}H NMR (300 MHz, DMSO-d6): 10.39 (s, 1H), 9.64 (s, 1H), 8.45 (s, 1H), 7.98 (d, J = 8.4 Hz, 2H), 7.43 (d, J = 8.4 Hz, 2H), 7.16 (d, J = 7.8 Hz, 1H), 6.96 (m, 1H), 6.80 (m, 1H), 6.62 (m, 1H), 6.41 (s, 1H), 5.51 (s, 2H), 4.90 (s, 2H), 2.27 (s, 3H). ^{13}C (125 MHz, DMSO-d_6): 174.23, 164.88, 152.76, 152.15, 150.69, 143.05, 142.22, 139.71, 134.19, 129.60, 128.20, 127.48, 126.44, 123.14, 118.32, 116.15, 116.02, 46.14, 22.08. HRMS (ESI) for $C_{23}H_{20}ClN_9O$ ($M+H^+$): calcd, 474.1558; found, 474.1554.

Synthesis of N-(2-aminophenyl)-4-((2-chloro-4-((3-chloro-4-fluorophenyl)amino)-7H-pyrrolo[2,3-d]pyrimidin-7-yl)methyl)benzamide (12)

The title compound **12** was synthesized in 61 % yield from compound **45** using benzene-1,2-diamine in a manner similar to that described for the synthesis of compound **7**. mp: 196 -197 °C; ^{1}H NMR (300 MHz, CD_3OD): 8.24 (dd, J =2.7 Hz and 6.9 Hz, 1H), 7.99 – 8.04 (m, 3H), 7.80 (m, 1H), 7.60 (d, J = 8.4 Hz, 2H), 7.24 (d, J = 7.5 Hz, 1H), 7.13 (m, 1H), 6.86 (dd, J = 1.5 and 8.1 Hz, 1H), 6.88 (d, J = 3.6 Hz, 1H), 6.79 (m, 1H), 6.62 (d, J = 3.9 Hz, 1H), 4.81 (s, 2H). ^{13}C (75 MHz, DMSO-d_6): 165.40, 155.39, 152.84, 152.61, 151.40, 143.62, 143.23, 140.10, 136.63, 134.74, 128.76, 127.76, 127.17, 127.01, 123.63, 122.98, 121.92, 119.52, 119.36, 117.30, 117.01, 116.68, 116.54, 46.76. HRMS (ESI) for $C_{26}H_{20}Cl_2FN_6O$ ($M+H^+$): found, 521.2605; MS (ESI): 521.25 [M+H], 519.20 [M-H].

Synthesis of 4-((2-amino-6-((3-chloro-4-fluorophenyl)amino)-9H-purin-9-yl)methyl)-N-(2-aminophenyl) benzamide (14)

The title compound **14** was synthesized in 68 % yield from compound **46** using benzene-1,2-diamine in a manner similar to that described for the synthesis of compound **7**. mp: 160 -162 °C; ^{1}H NMR (300 MHz, DMSO-d6): 9.69 (s, 1H), 9.62 (s, 1H), 8.30 (dd, J = 2.7 Hz and 6.9 Hz, 1H), 7.95 – 8.02 (m, 4H), 7.29 – 7.39 (m, 3H), 7.17 (d, J = 7.8 Hz, 1H), 6.98 (m, 1H), 6.77 (dd, J = 1.2 and 8.1 Hz, 1H), 6.60 (m, 1H), 6.28 (s, 2H), 5.36 (s, 2H), 4.89 (s, 2H). ^{13}C (125 MHz, DMSO-d_6): 164.93, 162.26, 159.96, 152.06, 151.95, 151.45, 143.03, 140.59, 138.40,

137.70, 133.94, 128.10, 126.93, 126.45, 123.17, 121.09, 120.13, 118.59, 116.12, 116.03, 113.63, 45.37. HRMS (ESI) for $C_{25}H_{20}ClFN_8O$ ($M+H^+$): calcd, 503.1511; found, 503.1507.

Synthesis of 4-((2-amino-6-((3,5-dimethoxyphenyl)amino)-9H-purin-9-yl)methyl)-N-(2-aminophenyl)benzamide (15)

The title compound **15** was synthesized in 69 % yield from compound **47** using benzene-1,2-diamine in a manner similar to that described for the synthesis of compound **7**. mp: 260-262 °C; ^{1}H NMR (300 MHz, DMSO-d6): 10.57 (s, 1H), 9.64 (s, 1H), 7.95 (s, 1H), 7.91 (d, J = 8.0 Hz, 2H), 7.32 (d, J = 8.0 Hz, 2H), 7.30 (d, J = 1.5 Hz, 2H), 7.12 (d, J = 7.5 Hz, 1H), 6.93 (m, 1H), 6.74 (d, J = 8.0 Hz, 1H), 6.56 (t, J = 7.5 Hz, 1H), 6.14 (s, 2H), 6.10 (t, J = 2.5 Hz, 1H), 5.31 (s, 2H), 4.84 (s, 2H), 3.71 (s, 6H). ^{13}C (125 MHz, DMSO-d_6): 164.94, 160.19, 159.98, 152.30, 151.86, 143.03, 141.88, 140.65, 138.15, 133.92, 128.09, 126.92, 126.59, 126.43, 123.17, 116.17, 116.03, 113.81, 98.36, 54.98, 45.35. HRMS (ESI) for $C_{27}H_{26}N_8O_3$ ($M+H^+$): calcd, 511.2206; found, 511.2203.

Synthesis of 4-((2-amino-4-((3-chloro-4-fluorophenyl)amino)-7H-pyrrolo[2,3-d]pyrimidin-7-yl)methyl)-N-(2-aminophenyl)benzamide (16)

The title compound **16** was synthesized in 63 % yield from compound **48** using benzene-1,2-diamine in a manner similar to that described for the synthesis of compound **7**. mp: 201 - 203 °C; ^{1}H NMR (300 MHz, DMSO-d6): 9.62 (s, 1H), 9.16 (s, 1H), 8.30 (dd, J = 2.4 Hz and 6.9 Hz, 1H), 7.82 – 7.97 (m, 4H), 7.50 (d, J = 8.4 Hz, 2H), 7.31 (m, 1H), 7.11 – 7.20 (m, 2H), 6.98 (m, 1H), 6.79 – 6.84 (m, 2H), 6.58 -6.64 (m, 2H), 4.90 (s, 2H), 4.64 (d, J = 6.3 Hz, 2H). ^{13}C (75 MHz, DMSO-d_6): 163.10, 160.14, 156.46, 151.31, 148.21, 143.03, 140.92, 136.07, 130.49, 125.48, 124.48, 124.40, 124.25, 121.26, 118.37, 117.33, 117.25, 116.23, 114.30, 114.12, 113.99, 96.54, 95.05, 42.15. HRMS (ESI) for $C_{26}H_{21}ClFN_7O$ ($M+H^+$) : calcd, 502.1558; found, 502.1556.

Synthesis of methyl 4-((2-chloro-9H-purin-6-yl)amino)benzoate (49)

The title compound **49** was synthesized in 77 % yield from compound **19** using methyl 4-aminobenzoate in a manner similar to that described for the synthesis of compound **31**. ^{1}H NMR (300 MHz, CD_3OD): 8.51 (s, 1H), 8.08 (d, J = 8.7 Hz, 2H), 7.89 (d, J = 8.7 Hz, 2H), 3.89 (s, 3H).

Synthesis of 4-((2-chloro-9H-purin-6-yl)amino)benzoic acid (50)

The title compound **50** was synthesized in 97 % yield from compound **49** in a manner similar to that described for the synthesis of compound **27**. ^{1}H NMR (300 MHz, CD_3OD): 8.52 (s, 1H), 8.16 (d, J = 8.7 Hz, 2H), 7.99 (d, J = 8.7 Hz, 2H).

Synthesis of 4-((2-chloro-9H-purin-6-yl)amino)-N-((tetrahydro-2H-pyran-2-yl)oxy)benzamide (51)

The title compound **51** was synthesized in 69 % yield from compound **50** using NH_2OTHP in a manner similar to that described for the synthesis of compound **7**. ^{1}H NMR (300 MHz, CD_3OD): 8.59 (s, 1H), 8.06 (d, J = 8.7 Hz, 2H), 7.97 (d, J = 8.7 Hz, 2H), 5.11 (s, 1H), 3.79 (m, 1H), 3.62 (m, 1H), 1.52 – 1.59 (m, 6H).

Synthesis of methyl 4-((2-chloro-6-((4-(((tetrahydro-2H-pyran-2-yl)oxy)carbamoyl)phenyl)amino)-9H-purin-9-yl)methyl)benzoate (52)

The title compound **52** was synthesized in 62 % yield from compound **51** using methyl 4-(bromomethyl) benzoate in a manner similar to that described for the synthesis of compound **23**. ^{1}H NMR (300 MHz, CD_3OD): 8.21 (s, 1H), 8.15 – 8.19 (m, 4H), 7.78 (d, J = 8.7 Hz, 2H), 7.39 (d, J = 8.1 Hz, 2H), 5.46 (s, 2H), 5.15 (bs, 1H), 3.92 (s, 3H), 3.89 (m, 1H), 3.67 (m, 1H), 1.55 – 1.61 (m, 6H).

Synthesis of 4-((2-chloro-6-((4-(((tetrahydro-2H-pyran-2-yl)oxy)carbamoyl)phenyl)amino)-9H-purin-9-yl)methyl)benzoic acid (53)

The title compound **53** was synthesized in 93 % yield from compound **52** in a manner similar to that described for the synthesis of compound **27**. ^{1}H NMR (300 MHz, CD_3OD): 8.25 (s, 1H), 8.11 – 8.14 (m, 4H), 7.81 (d, J = 8.7 Hz, 2H), 7.42 (d, J = 8.1 Hz, 2H), 5.46 (s, 2H), 5.15 (bs, 1H), 3.87 (m, 1H), 3.66 (m, 1H), 1.55 – 1.61 (m, 6H).

Synthesis of N-(2-aminophenyl)-4-((2-chloro-6-((4-(((tetrahydro-2H-pyran-2-yl)oxy)carbamoyl)phenyl)amino)-9H-purin-9-yl)methyl)benzamide (54)

The title compound **54** was synthesized in 53 % yield from compound **53** using benzene-1,2-diamine in a manner similar to that described for the synthesis of compound **7**. ^{1}H NMR (300 MHz, CD_3OD): 8.29 (s, 1H), 8.00 – 8.06 (m, 4H), 7.85 (d, J = 8.7 Hz, 2H), 7.47 (d, J = 8.1 Hz, 2H), 7.12 (d, J = 7.8 Hz, 1H), 6.94 (m, 1H), 6.82 (d, J = 7.8 Hz, 1H), 6.68 (m, 1H), 5.57 (s, 2H), 5.10 (bs, 1H), 3.91 (m, 1H), 3.66 (m, 1H), 1.59 – 1.66 (m, 6H).

Synthesis of N-(2-aminophenyl)-4-((2-chloro-6-((4-(hydroxycarbamoyl)phenyl)amino)-9H-purin-9-yl)methyl)benzamide (9)

To the stirring solution of compound **54** (500 mg, 0.84 mmol) in CH_3OH (10 mL) was added 10% aq. TFA (2 mL). The reaction was stirred at room temperature for 5 h and the reaction mixture was concentrated under reduced pressure to give off white precipitates, which were

recrystallized from CH3OH to afford the to give the title compound **9** in 52% yield; mp: 210 -212 °C; ^{1}H NMR (300 MHz, DMSO): 11.15 (s, 1H), 10.60 (s, 1H), 9.67 (s, 1H), 8.54 (s, 1H), 7.95 - 7.97 (m, 4H), 7.77 (d, J = 8.7 Hz, 2H), 7.45 (d, J = 8.1 Hz, 2H), 7.18 (d, J = 7.8 Hz, 1H), 6.99 (m, 1H), 6.80 (d, J = 7.8 Hz, 1H), 6.63 (m, 1H), 5.54 (s, 2H). ^{13}C (125 MHz, DMSO-d_6): 171.43, 164.91, 163.94, 152.36, 152.13, 150.54, 142.73, 142.63, 139.61, 134.20, 129.60, 128.23, 127.98, 126.95, 126.49, 123.36, 122.48, 120.28, 119.07, 118.17, 116.50, 46.24. HRMS (ESI) for $C_{26}H_{21}ClN_8O_3$ ($M+H^+$): calcd, 529.1503; found, 529.1498.

Synthesis of N^4-methyl-7H-pyrrolo[2,3-d]pyrimidine-2,4-diamine (55)

To the solution of compound **22** (1 g, 5.9 mmol) in butanol (10 mL), methylamine (3 mL, 40 % wt in H_2O) was added. The reaction mixture was heated at 70 °C for 3 h. Water was added to the reaction mixture and butanol layer was separated. The organic layer was concentrated under reduced pressure. The resulting residue was used as such without purification for further reaction. 1H NMR (DMSO-d_6): 10.63 (s, 1H), 6.93 (d, J = 4.5 Hz), 6.62 (dd, J = 1.8 Hz, 1H), 6.28 (dd, J = 1.5 and 3.3 Hz, 1H), 5.43 (s, 2H), 2.88 (d, J = 4.5 Hz).

Synthesis of 1-(4-(methylamino)-7H-pyrrolo[2,3-d]pyrimidin-2-yl)-3-(2,4,6-trichloro-3,5-dimethoxyphenyl)urea (56)

A mixture of compound **55** (0.700 mg, 4.29 mmol), triphosgene (2.54 g, 8.55 mmol) and trimethylamine in THF was stirred at room temperature for 3 h. The solvent was evaporated under reduced pressure and the residue was dissolved in toluene. To this solution, 2,4,6-trichloro-3,5-dimethoxyaniline (1.1 g, 4.29 mmol) was added and the reaction mixture was refluxed for 3h. The reaction was quenched with H_2O and extracted with EtOAc (50 mL x 3). The combined organic layer was dried over anhydrous $MgSO_4$, concentrated under reduced pressure and purified by silica gel chromatography (ethyl acetate) to give compound **56** in 73 % yield; ^{1}H NMR (300 MHz, DMSO-d6): 11.98 (s, 1H), 11.34 (s, 1H), 9.49 (s, 1H), 7.75 (bs, 1H), 6.94 (dd, J = 2.1 Hz and 3.3 Hz, 1H), 6.49 (dd, J = 1.8 and 3.3 Hz), 3.89 (s, 6H), 2.94 (d, J = 3.0 Hz, 3H).

Synthesis of methyl 4-((4-(methylamino)-2-(3-(2,4,6-trichloro-3,5-dimethoxyphenyl)ureido)-7H-pyrrolo[2,3-d]pyrimidin-7-yl)methyl)benzoate (57)

The title compound **57** was synthesized in 66 % yield from compound **56** and methyl 4-(bromomethyl)benzoate in an manner similar to that described for the synthesis of compound **23**. ^{1}H NMR (300 MHz, CD_3OD): 7.81 (d, J = 8.7 Hz, 2H), 7.31 (d, J = 8.7 Hz, 2H), 7.16 (d, J = 3.3 Hz, 1H), 6.61 (bs, 1H), 5.32 (s, 2H), 3.89 (s, 6H), 3.83 (s, 3H), 2.93 (s, 3H).

Synthesis of 4-((4-(methylamino)-2-(3-(2,4,6-trichloro-3,5-dimethoxyphenyl)ureido)-7H-pyrrolo[2,3-d]pyrimidin-7-yl)methyl)benzoic acid (58)

The title compound **58** was synthesized in 97 % yield from compound **57** in a manner similar to that described for the synthesis of compound **27**. ^{1}H NMR (300 MHz, CD_3OD): 7.84 (d, J = 8.1 Hz, 2H), 7.26 (d, J = 8.1 Hz, 2H), 7.12 (d, J = 3.3 Hz, 1H), 6.63 (bs, 1H), 5.37 (s, 2H), 3.88 (s, 6H), 2.93 (s, 3H).

Synthesis of N-(2-aminophenyl)-4-((4-(methylamino)-2-(3-(2,4,6-trichloro-3,5-dimethoxyphenyl)ureido)-7H-pyrrolo[2,3-d]pyrimidin-7-yl)methyl)benzamide (18)

The title compound **18** was synthesized in 57 % yield from compound **58** in a manner similar to that described for the synthesis of compound **13**. ^{1}H NMR (300 MHz, DMSO-d_6): 9.58 (s, 1H), 9.53 (s, 1H), 7.84 (d, J = 8.1 Hz, 2H), 7.26 (d, J = 8.1 Hz, 2H), 7.12 - 7.16 (m, 2H), 6.98 (m, 1H), 6.77 (d, J = 8.1 Hz, 1H), 6.57 – 6.63 (m, 2H), 5.37 (s, 2H), 4.87 (s, 2H), 3.88 (s, 6H), 2.93 (s, 3H). ^{13}C (125 MHz, DMSO-d_6): 174.24, 164.81, 162.26, 153.12, 151.72, 151.46, 151.41, 143.03, 141.35, 133.81, 133.61, 129.60, 127.89, 126.85, 126.58, 126.42, 124.16, 123.19, 123.08, 121.76, 116.19, 116.04, 60.70, 47.15. MS (ESI) for $C_{30}H_{28}Cl_3N_8O_4$ ($M+H^+$): calcd, 669.12; found, 669.15

4.2 Biology

4.2.1. Cell culture

The human MDA-MB-231 breast cancer cell line and HepG2 liver cancer cell line were cultured in DMEM medium. The human YCC11 and YCC3/7 gastric cancer cell lines and MCF-7 breast cancer cell line were cultured in αMEM medium. The human K-562, KG-1 and THP-1 leukemia cell lines were cultured in IMDM, RPMI and RPMI containing 0.05 mM of 2-mercaptoethanol, respectively. All medium containing 10% fetal bovine serum (FBS) and 1% penicillin/streptomycin/glutamine (PSG). All cell lines described above were cultured at 37□ in a humidified atmosphere 5% CO_2. The human MDA-MB-468 breast cancer cell line was cultured in L-15 medium with 10% FBS and 1%PSG at 37 □ in a humidified atmosphere without CO_2.

4.2.2. Chemicals and antibodies

MS-275 and the derivatives were synthesized by Dr. Jing-Ping Liou as described above. Chidamide was purchased from Selleckchem. The compounds were dissolved in dimethylsulfoxide (DMSO) and then stored at −20℃ with limited freeze-thaw cycles. Propidium iodide, RNase A and 3-(4,5-Dimethylthiazol-2-yl)-2,5-diphenyltetrazolium bromide (MTT) were purchased from Sigma. 3-(4,5-Dimethylthiazol-2-yl)-5-(3-carboxymethoxyphenyl)-2-(4-sulfophenyl)-2H-tetrazolium

(MTS) was purchased from Biovision. Primary antibodies: mouse anti-Caspase-3 (NB100-56708; Novus); mouse anti-Caspase-8 (9746; Cell Signaling); rabbit anti-Histone 3 (ab1791; Abcam); rabbit anti-acetyl-Histone 3 lysine 9 (07-352; Millipore); rabbit anti-Histone 4 (ab10158; Abcam); rabbit anti-acetyl-Histone 4 lysine 5/8/12/16 (06-866; Millipore); mouse anti-p21 (sc-6246; Santa Cruz); rabbit anti-p53 (sc-6243; Santa Cruz); rabbit anti-PARP-1 (sc-7150; Santa Cruz); rabbit anti-SMC3 (A300-060A; Bethyl); mouse anti-acetyl-SMC3 lysine 105/106 (MABE1073; Millipore); mouse anti-α-tubulin (T5168; Sigma); mouse anti-acetyl-α-Tubulin lysine 40 (T7451; Sigma).

4.2.3. MTT assays

Attached cells grown on 96-well plates were treated with indicated compounds. After 72 hours, cells were incubated with medium containing 1 mg/ml MTT for 4 hours. The precipitated formazan crystals were then dissolved with 100 μl DMSO, followed by mesuremnet of absorbance at 490 nm. The 50% of growth inhibitory concentration (IC_{50}) was calculated by CompuSyn software.

4.2.4. MTS assays

Suspension cells grown on 96-well plates were treated with indicated compounds. After 72 hours, cells were incubated with medium containing 0.2 mg/ml MTS for 2 hours, and followed

by mesuremnet of absorbance at 490 nm. The 50% of growth inhibitory concentration (IC_{50}) was calculated by CompuSyn software.

4.2.5 HDAC enzymes inhibition assays

Enzyme inhibition assays were performed by the Reaction Biology Corporation, Malvern, PA. (http://www.reactionbiology.com). The substrate for HDAC1-10 is a fluorogenic peptide derived from p53 residues 379–382 [RHKK(Ac)]. Compounds were dissolved in DMSO and tested in 10-dose IC_{50} mode with 3-fold serial dilution starting at 10 μM Trichostatin A (TSA) was the reference.

4.2.6 Molecular Docking

Molecular docking analysis of compound **14** was performed using LeadI [56]. Structures of HDAC1 (PDB ID: 5ICN), HDAC4 (PDB ID: 4CBT), HDAC6 (PDB ID: 5EDU) and HDAC8 (PDB ID: 5VI6) were obtained from the Protein Data Bank [57]. A radius of 12 Å from the co-crystal ligand was set as the binding site. A hybrid enthalpy and entropy docking strategy approach was used. The maximum number of solutions for both the iteration and fragmentation was set at 300.

The molecular dynamics (MD) simulation was performed after docking the ligand, compound **14**, into HDAC1 (PDB ID: 5ICN). The MD ensures a degree of reproducibility of docking results and was performed in Pipeline Pilot [58]. The MD simulations was performed using the

CHARMm force field. A simulation time of 10,000 ps was used at a target temperature of 300K. The time interval during the production process was set to 100 ps. All other parameters and settings were used with default values. Finally, the stability of the protein-ligand complex from the MD was compared by superimposing its pose with that of its docked pose.

4.2.7 Western blot analysis

Cell extracts were harvested using 1x Laemmli Sample Buffer (60 mM Tris (pH 6.8), 2% SDS and 10% glycerol) and protein concentration was determined by BCA Protein Assay Kit (Thermo scientific). Equal protein amounts were separated by 12% SDS-PAGE and then transferred onto nitrocellulose membrane. The membranes were blocked with 5% skim milk and the indicated proteins were then probed with specific primary antibodies, followed by detection with horseradish peroxidase (HRP)-conjugated secondary antibodies (Jackson ImmunoResearch) with enhanced chemiluminescence (ECL) substrates (Bio-Rad).

4.2.8. Flow cytometry

Cells were fixed with ice-cold ethanol (70%, v/v) at 4℃ for at least 15 minutes. Fixed cells were then washed with cold PBS containing 1% FBS and incubated in propidium iodide (PI) staining buffer (PBS with 0.05 mg/ml PI and 0.25 mg/ml RNase A) at 37℃ for 30 minutes. DNA content was measured by BD FACSCalibur and cell cycle profiles were plot using FlowJo software.

4.2.9 Xenograft mouse model

The human breast cancer cells MDA-MB-231 used for implantation were injected subcutaneously (s.c.) with $1x10^7$ cells into 10 week-old male BALB/c nude mice. After tumor volume reached about 80-100 mm^3, mice were divided into 4 groups (n = 4). Mice were treated with vehicle control, 10 mg/kg Taxol (intravenous injection; every other day), 25 mg/kg or 50mg/kg compound **14** (intraperitoneal injection; every day; dissolved in 5% DMSO, 5% cremphor and 90% Dextrose). Tumor volumes were monitored daily at week one and then twice weekly until the tumor volumes of the control group approached the maximum. Tumor volume was calculated from ($width^2$ x length)/2. Animal experiments were performed in accordance with relevant guidelines and regulations and followed ethical standards. Protocols have been reviewed and approved by Animal Use and Management Committee of Taipei Medical University (AC-2018-0183). Statistical analysis was performed using an SPSS statistical soft-ware program (SPSS Inc., Chicago, IL). All data represent the mean ± S.E.M. from at least three independent experiments. The efficacy of compound **14** and Taxol were performed by Generalized estimating equations.

Acknowledgements

We thank Dr. Sun Young Rha (Songdang Institute for Cancer Research) for providing YCC cell lines and Nian-Zhe Lee (Master Program in Clinical Pharmacogenomics and Pharmacoproteomics, TMU) for assistance. We also appreciate the technical supports provide by the TMU Core Facility. This research was supported by the Ministry of Science and Technology, Taiwan (grant no. MOST 107-2113-M-038 -001; MOST 108-2113-M-038-005).

References

[1] T. Jenuwein, C.D. Allis, Translating the histone code, Science 293 (2001) 1074 - 1080.

[2] a) J. Taunton, C.A. Hassig, S.L. Schreiber, A mammalian histone deacetylase related to the yeast transcriptional regulator Rpd3p, Science 272 (1996) 408−411. b) C.A. Hassig, S.L. Schreiber, Nuclear histone acetylases and deacetylases and transcriptional regulation: HATs off to HDACs, Curr. Opin. Chem. Biol. 1 (1997) 300−308. c) S. Minucci, P.G. Pelicci, Histone deacetylase inhibitors and the promise of epigenetic (and more) treatments for cancer, Nat. Rev. Cancer 6 (2006) 38-51. d) M. Paris, M. Porcelloni, M. Binaschi, D. Fattori, Histone deacetylase inhibitors: from bench to clinic, J. Med. Chem. 51 (2008) 1505-1529. e). A.G. Kazantsev, L.M. Thompson, Therapeutic application of histone deacetylase inhibitors for central nervous system disorders, Nat. Rev. Drug Discov. 7 (2008) 854-868. f) R. Glauben, E. Sonnenberg, M. Zeitz, B. Siegmund, HDAC inhibitors in models of inflammation-related

tumorigenesis, Cancer Lett. 280 (2009) 154-159. g) F. Thaler, S. Minucci, Next generation histone deacetylase inhibitors: the answer to the search for optimized epigenetic therapies? Expert Opin. Drug Disc. 6 (2011) 393-404. h) M. Federico, L. Bagella, Histone deacetylase inhibitors in the treatment of hematological malignancies and solid tumors, J. Biomed. Biotechnol. 2011 (2011) 475641. i) D.S. Reddy, X. Wu, V.M. Golub, W.M. Dashwood, R.H. Dashwood, Measuring Histone Deacetylase Inhibition in the Brain, Curr. Protoc. Pharmacol. 81 (2018) e41.

[3] a) I. Naldi, M. Taranta, L. Gherardini, G. Pelosi, F. Viglione, S. Grimaldi, L. Pani, C. Cinti, Novel Epigenetic Target Therapy for Prostate Cancer: A Preclinical Study, PLoS One 9 (2014), 9810. b) T. Jenuwein, C.D. Allis, Translating the histone code, Science 293 (2001) 1074−1080. c) C.A. Hassig, S.L. Schreiber, Nuclear histone acetylases and deacetylases and transcriptional regulation: HATs off to HDACs, Curr. Opin. Chem. Biol. 1 (1997) 300−308. d) H.Y. Lee, K. Nepali, F.I. Huang, C.Y. Chang, M.J. Lai, Y.H. Li, H.L. Huang, C.R. Yang, J.P. Liou, (N Hydroxycarbonyl benzylamino) quinolines as Selective Histone Deacetylase 6 Inhibitors Suppress Growth of Multiple Myeloma *in Vitro* and in Vivo, J. Med. Chem. 61 (2018) 905-917.

[4] a) C.M. Marson, Histone deacetylase inhibitors: design, structure− activity relationships and therapeutic implications for cancer, Anti- Cancer Agents Med. Chem. 9 (2009) 661−692. b) S.

Minucci, G. Pelicci, Histone deacetylase inhibitors and the promise of epigenetic (and more) treatment for cancer, Nat. Rev. Canc. 6 (2006) 38−51.

[5] a) A. Mai, Small-molecule chromatin-modifying agents: therapeutic applications, Epigenomics 2 (2010) 307−324. b) R. Benedetti, M. Conte, L. Altucci, Targeting HDACs in diseases:

where are we? Antioxid. Redox Signaling 23 (2014) 99–126. c) M. Kirschbaum, P. Frankel, L. Popplewell, J. Zain, M. Delioukina, V. Pullarkat, D. Matsuoka, B. Pulone, A.J. Rotter, I. Espinoza-Delgado, Phase II study of vorinostat for treatment of relapsed or refractory indolent non-Hodgkin's lymphoma and mantle cell lymphoma, J. Clin. Oncol. 29 (2011) 1198 - 1203. c) L.M. Butler, D.B. Agus, H.I. Scher, B. Higgins, A. Rose, C. Cordon-Cardo, H.T. Thaler, R.A. Rifkind, P.A. Marks, V.M. Richon, Suberoylanilide hydroxamic acid, an inhibitor of histone deacetylase, suppresses the growth of prostate cancer cells in vitro and in vivo, Cancer Res. 60 (2000) 5165-5170. d) V. Lakshmikanthan, I. Kaddour, Djebbar, R. W. Lewis, M. V. Kumar, SAHA sensitized prostate cancer cells to TNFa-related apoptosis inducing ligand(TRAIL): mechanisms leading to synergistic apoptosis, Int. J. Can. 119 (2006) 221 - 228. e) J.P. Huang, K. Ling, EZH2 and histone deacetylase inhibitors induce apoptosis in triple negative breast cancer cells by differentially increasing H3 Lys^{27}acetylation in the *BIM* gene promoter and enhancers, Oncol Lett. 14 (2017) 5735-5742. f) D. Carlisi, B. Vassallo, M. Lauricella, S.

Emanuele, A. D'Anneo, E. Di Leonardo, P. Di Fazio, R. Vento, G. Tesoriere, Histone deacetylase inhibitors induce in human hepatoma HepG2 cells acetylation of p53 and histones in correlation with apoptotic effects, Int. J. Oncol. 32 (2008) 177 - 84. g) P. Fedele, O. Laura, S. Cinieri, Targeting triple negative breast cancer with histone deacetylase inhibitors, Expert Opin. Investig. Drugs 26 (11) (2017) 1199-1206. g) R.L. Piekarz, R.W. Robey, Z. Zhan, G. Kayastha, A. Sayah, A.H. Abdeldaim, S. Torrico, S.E. Bates, T-cell lymphoma as a model for the use of histone deacetylase inhibitors in cancer therapy: impact of depsipeptide on molecular markers, therapeutic targets, and mechanisms of resistance, Blood 103 (2004) 4636−4643.

[6] a) B. Zhang, J. Liu, D. Gao, X. Yu, J. Wang, X. Lei, A fluorine scan on the Zn^{2+}-binding thiolate side chain of HDAC inhibitor largazole: Synthesis, biological evaluation, and molecular modeling. Eur. J. Med. Chem. 182 (2019) 111672. b) X. Li, Y.K. Peterson, E.S. Inks, R.A. Himes, J. Li, Y. Zhang, X. Kong, C.J. Chou, Class I HDAC Inhibitors Display Different Antitumor Mechanism in Leukemia and Prostatic Cancer Cells Depending on Their p53 Status. J. Med. Chem. 61 (2018) 2589-2603. c) J.J. McClure, C. Zhang, E.S. Inks, Y.K. Peterson, J. Li, C.J. Chou, Development of Allosteric Hydrazide-Containing Class I Histone Deacetylase Inhibitors for Use in Acute Myeloid Leukemia, J. Med. Chem. 21 (2016) 9942-9959. d) C.M. Marson, C.J. Matthews, S.J. Atkinson, N. Lamadema, N.S. Thomas, Potent and Selective Inhibitors of Histone Deacetylase□3 Containing Chiral Oxazoline Capping Groups and a

N□(2-Aminophenyl)-benzamide Binding Unit, J. Med. Chem. 58 (2015) 6803-18. e) V. Krieger, A. Hamacher, F. Cao, K. Stenzel, C. G. W. Gertzen, L. Schäker-Hübner, T. Kurz, H. Gohlke, F. J. Dekker, M. U. Kassack, F.K. Hansen, Synthesis of Peptoid-Based Class I□Selective Histone Deacetylase Inhibitors with Chemosensitizing Properties, J. Med. Chem. 62 (2019) 11260-11279. f) M. Ahmad, A.A. Mushtaq, J. A. Bhat, B. Kumar, A. Rouf, N. Capalash, M.J. Mintoo, A. Kumar, P. Mahajan, D. M. Mondhe, A. Nargotra, P. R. Sharma, M. A. Zargar, R.A. Vishwakarma, B. A. Shah, S. C. Taneja, A. Hamid, Exploring Derivatives of Quinazoline Alkaloid L□Vasicine as Cap Groups in the Design and Biological Mechanistic Evaluation of Novel Antitumor Histone Deacetylase Inhibitors, J. Med. Chem. 60 (2017) 3484-3497. g) Y. Yao, Z. Tu, C. Liao, Z. Wang, S. Li, H. Yao, Z. Li, S. Jiang, Discovery of Novel Class I Histone Deacetylase Inhibitors with Promising in Vitro and in Vivo Antitumor Activities, J. Med. Chem. 58 (2015) 7672-80. h) X. Li, E.S. Inks, X. Li, J. Hou, C. J. Chou, J. Zhang, Y. Jiang, Y. Zhang, W. Xu, Discovery of the first N□Hydroxycinnamamide-based histone deacetylase 1/3 Dual Inhibitors with Potent Oral Antitumor Activity, J. Med. Chem. 57 (2014) 3324-41. i) S. Valente, D. Trisciuoglio, T. De Luca, A. Nebbioso, D. Labella, A. Lenoci, C Bigogno, G. Dondio, M. Miceli, G. Brosch, D. D. Bufalo, L. Altucci, A. Mai,1,3,4-Oxadiazole-Containing Histone Deacetylase Inhibitors:Anticancer Activities in Cancer Cells, J. Med. Chem. 57 (2014) 6259-65.j) C. M. Marson, C. J. Matthews, E. Yiannaki,

S. J. Atkinson, P. E. Soden, L. Shukla, N. Lamadema, N. S. B. Thomas, Discovery of Potent, Isoform-Selective Inhibitors of Histone Deacetylase Containing Chiral Heterocyclic Capping Groups and a N□(2-Aminophenyl) benzamide Binding Unit, *J. Med. Chem.* 56 (2013) 6156-6174.

7. a) H. A.bdelkarim, R. Neelarapu, A. Madriaga, A. S. Vaidya, I. Kastrati, B. Karumudi, Y.T. Wang, T.Y. Taha, R.J. G.Thatcher, J. Frasor, P. A. Petukhov, Design, Synthesis, Molecular Modeling, and Biological Evaluation of Novel Amine-based Histone Deacetylase Inhibitors, ChemMedChem. 12 (2017) 2030-2043. b) Z. Noor, N. Afzal, S. Rashid, Exploration of Novel Inhibitors for Class I Histone Deacetylase Isoforms by QSAR Modeling and Molecular Dynamics Simulation Assays, PLOS ONE 10 (2015) e0143155. c). C. Chen, X. Hou, G. Wang, W. Pan, X. Yang,Y. Zhang, H. Fang, Design, synthesis and biological evaluation of quinoline derivatives as HDAC class I inhibitors, Eur. J. Med. Chem. 133 (2017) 11-23. d) F. Yun, C. Cheng, S. Ullah, J. He, M. R. Zahi, Q. Yuan, Thioether-based 2-aminobenzamide derivatives: Novel HDAC inhibitors with potent in vitro and in vivo antitumor activity, Eur. J. Med. Chem. 176 (2019) 195-207. e) G. Cheng, Z. Wang, J. Yang, Y. Bao, Q. Xu, L. Zhao, D. Liu, Design, synthesis and biological evaluation of novel indole derivatives as potential HDAC/BRD4 dual inhibitors and anti-leukemia agents, Bioorg. Chem. 84 (2019) 410-417. f) A. B. Farag, H. A. Ewida, M. S. Ahmed, Design, synthesis, and biological evaluation of novel

amide and hydrazide based thioether analogs targeting Histone deacteylase (HDAC) enzymes, Eur. J. Med. Chem. 148 (2018) 73-85. g). R. Cincinelli, V. Zwick, L. Musso, V. Zuco, M. De Cesare, F. Zunino, C. Simoes-Pires, A. Nurisso, G. Giannini, M. Cuendet, S, Dallavalle, Biphenyl-4-yl-acrylohydroxamic acids: Identification of a novelindolyl-substituted HDAC inhibitor with antitumor activity, Eur. J. Med. Chem. 112 (2016) 99-105. h). R. M. Okasha, M. Alsehli, S. Ihmaid, S.S. Althagfan, M.S.A. El-Gaby,H.E.A. Ahmed, T.H.Afifi, First example of Azo-Sulfa conjugated chromene moieties: Synthesis, characterization, antimicrobial assessment, docking simulation as potent class I histone deacetylase inhibitors and antitumor agents, Bioorg. Chem. 92 (2019) 103262. i) X. Liang, M. Deng, C. Zhang, F. Ping, H. Wang, Y Wang, Z. Fan, X. Ren, X. Tao, T. Wu, J. Xu, B. Cheng, J. Xia, Combined class I histone deacetylase and mTORC1/C2 inhibition suppresses the initiation and recurrence of oral squamous cell carcinomas by repressing SOX2, Canc. Lett. 454 (2019) 108-119. j) S. Hiranaka, Y. Tega, K. Higuchi, T. Kurosawa, Y. Deguchi, M. Arata,A. Ito, M. Yoshida, Y. Nagaoka, T. Sumiyoshi, Design, Synthesis, and Blood−Brain Barrier Transport Study of Pyrilamine Derivatives as Histone Deacetylase Inhibitors, ACS Med. Chem. Lett. 9 (2018) 884-888.

8. a) J. Zang, X. Liang, Y. Huang, Y. Jia, X. Li, W. Xu, C. J. Chou, Y. Zhang, Discovery of Novel Pazopanib-Based HDAC and VEGFR Dual Inhibitors Targeting Cancer Epigenetics and Angiogenesis simultaneously, J. Med. Chem. 61 (2018) 5304-5322. b). J. Sun, J. Wang, X.

Wang, H.C. Liu, M. Zhang, Y. Liu, C. Zhang, Y. Su, Y. Shen, Y.Guo, A. Shen, M. Geng, Marine-derived chromopeptide A, a novel class I HDAC inhibitor, suppresses human prostate cancer cell proliferation and migration, J. Med. Chem. 61 (2018) 5304-5322. c). H. Zhijun, W. Shusheng, M. Han, L. Jianping, Q. Li-Sen, L. Dechun, Pre-clinical characterization of 4SC-202, a novel class I HDAC inhibitor, against colorectal cancer cells, Tumor Biology 37 (2016) 10257–10267. d). K. Zhang, Y. Yao, Z. Tu, C. Liao, Z. Wang, Y. Qiu, D. Chen, D.J. Hamilton, Z. Li, S. Jiang, Discovery of class I histone deacetylase inhibitors based on romidpesin with promising selectivity for cancer cells, Future Med Chem. 2019 Nov 29. doi: 10.4155/fmc-2019-0290. e). J. Zang, X. Liang, Y. Huang, Y. Jia, X. Li, W. Xu, C.J. Chou, Y. Zhang, Discovery of Novel Pazopanib-Based HDAC and VEGFR Dual Inhibitors Targeting Cancer Epigenetics and Angiogenesis Simultaneously, J. Med. Chem. 61 (2018) 5304-5322. f). J.H. Kalin, M. Wu, A. V. Gomez, Y. Song, J. Das, D. Hayward, N. Adejola, M. Wu, I. Panova, H. J. Chung, E. Kim, H.J. Roberts, J.M. Roberts, P. Prusevich, J.R. Jeliazkov, S.S.R. Burman, L. Fairall, C. Milano, A. Eroglu, C.M. Proby, A.T. Dinkova-Kostova, W.W. Hancock, J.J. Gray, J.E. Bradner, S. Valente, A. Mai, N.M. Anders, M.A. Rudek, Y. Hu, B. Ryu, J.W.R. Schwabe, A. Mattevi, R.M. Alani, P. A. Cole, Targeting the CoREST complex with dual histone deacetylase and demethylase inhibitors, Nat Commun. 9 (2018), 9(1), 53. g) A.J. Wilson, Y.Q. Cheng, D. Khabele, Thailandepsins are new small molecule class I HDAC

inhibitors with potent cytotoxic activity in ovarian cancer cells: a preclinical study of epigenetic ovarian cancer therapy, J. Ovarian Res. 5 (1) (2012) 12.

9. a) V.R. Pidugu, N. S. Yarla, S. R. Pedada, A. M. Kalle, A. Krishna Satya, Design and synthesis of novel HDAC8 inhibitory 2,5-disubstituted-1,3,4-oxadiazoles containing glycine and alanine hybrids with anti-cancer activity, Bioorg. Med. Chem. 21 (2016) 5611-5617. b). J.C. Wong, G. Tang, X. Wu, C. Liang, Z. Zhang, L. Guo, Z. Peng, W. Zhang, X. Lin, Z. Wang, J. Mei, J. Chen, S. Pan, N. Zhang, Y. Liu, M. Zhou, L. Feng, W. Zhao, S. Li, C. Zhang, M. Zhang, Y. Rong, T.G. Jin, X. Zhang, S. Ren, Y. J. R. Zhao, J. She, Y. Ren, C. Xu, D. Chen, J. Cai, S. Shan, D. Pan, Z. Ning, X. Lu, T. Chen, Y. He, Li, Chen, Pharmacokinetic Optimization of Class-Selective Histone Deacetylase Inhibitors and Identification of Associated Candidate Predictive Biomarkers of Hepatocellular Carcinoma Tumor Response, J. Med. Chem. 55 (2012), 8903-25 c). S. Hiranaka, Y. Tega, K. Higuchi, T. Kurosawa, Y. Deguchi, M. Arata, A. Ito, M. Yoshida, Y. Nagaoka, T. Sumiyoshi, Design, Synthesis, and Blood−Brain Barrier Transport Study of Pyrilamine Derivatives as Histone Deacetylase Inhibitors, ACS Med. Chem. Lett. 9 (2018) 884-888. d). S.A. Amin, P. Bhattacharya, S. Basak, S. Gayen, A. Nandy, A. Saha, Pharmacoinformatics study of Piperolactam A from Piper betle root as new lead for non-steroidal anti fertility drug development, Comput. Biol. Chem. 67 (2017) 213-224. e). H. Zhou, C. Wang C, T. Deng, R. Tao, W. Li, Novel urushiol derivatives as HDAC8 inhibitors:

rational design, virtual screening, molecular docking and molecular dynamics studies, J. Biomol. Struct. Dyn. 36 (2018) 1966-1978.

[10] A. Marks, Discovery and development of SAHA as an anticancer agent, Oncogene 26 (2007) 1351 - 1356.

[11] X. Qian, G. Ara, E. Mills, W.J. LaRochelle, H.S. Lichenstein, M. Jeffers, Activity of the histone deacetylase inhibitor belinostat (PXD101) in preclinical models of prostate cancer, Int. J. Canc. 122 (2008) 1400 - 1410.

[12] J.P. Laubach, P. Moreau, J.F. San-Miguel, P.G, Richardson, Panobinostat for the treatment of multiple myeloma, Clin. Cancer Res. 21 (2015) 4767 - 4773.

[13] M. Fournel, C. Bonfils, Y. Hou, T. Yan, M.C. Trachy-Bourget, A. Kalita, J. Liu, A.H.; Lu, N.Z. Zhou, M.F. Robert, J. Gillespie, J.J. Wang, H. Ste-Croix, J. Rahil, S. Lefebvre, O. Moradei, D. Delorme, A.R. MacLeod, J.M. Besterman, Z. Li, MGCD0103, a novel isotype-selective histone deacetylase inhibitor, has broad spectrum antitumor activity *in vitro* and *in vivo*, Mol. Cancer Ther. 7 (2008) 759 - 768.

[14] J. Knipstein, L. Gore, Entinostat for treatment of solid tumors and hematologic malignancies, Expert Opin. Invest. Drugs 20 (2011) 1455 - 1467.

[15] a) Z. Qiao, S. Ren, W. Li, X. Wang, M. He, Y. Guo, L. Sun, Y. He, Y. Ge, Q. Yu. Chidamide, a novel histone deacetylase inhibitor, synergistically enhances gemcitabine

cytotoxicity in pancreatic cancer cells, Biochem. Biophys. Res. Commun. 434 (2013) 95 - 101. b) R. Gu, T. Liu, X. Zhu, H. Gan, Z. Wu, J. Li, Development and validation of a sensitive HPLC-MS/MS method for determination of Chidamide (epidaza), a new benzamide class of selective histone deacetylase inhibitor, in human plasma and its clinical application, J. Chromatogr. B Anal. Technol. Biomed. Life Sci. 1000 (2015) 181 -186. c) X. Lu, Z. Ning, Z. Li, H. Cao, X. Wang, Development of Chidamide for peripheral T-cell lymphoma, the first orphan drug approved in China, Intractable Rare Dis. Res. 5 (2016) 185 - 191.

[16] Y. Shi, B. Jia, W. Xu, W. Li, T. Liu, P. Liu, W. Zhao, H. Zhang, X. Sun, H. Yang, X. Zhang, J. Jin, Z. Jin, Z. Li, L. Qiu, M. Dong, X. Huang, Y. Luo, X. Wang, X. Wang, J. Wu, J. Xu, P. Yi, J. Zhou, H. He, L. Liu, J. Shen, X. Tang, J. Wang, J. Yang, Q. Zeng, Z. Zhang, Z. Cai, X. Chen, K. Ding, M. Hou, H. Huang, X. Li, R. Liang, Q. Liu, Y. Song, H. Su, Y. Gao, L. Liu, J. Luo, L. Su, Z. Sun, H. Tan, H. Wang, J. Wang, S. Wang, H. Zhang, X. Zhang, D. Zhou, O. Bai, G. Wu, L. Zhang, Y. Zhang, Chidamide in relapsed or refractory peripheral T cell lymphoma: a multicenter real-world study in China, J. Hematol. Oncol. 10 (1) (2017) 69.

[17] a) X. Hu, L. Wang, L. Lin, X. Han, G. Dou, Z. Meng, Y. Shi, A phase I trial of an oral subtype-selective histone deacetylase inhibitor, Chidamide, in combination with paclitaxel and carboplatin in patients with advanced non-small cell lung cancer, Chin. J. Cancer Res. 28 (2016) 444 - 451 b) S. Yang, P. Nan, C. Li, F. Lin, H. Li, T. Wang, C. Zhou, X. Zhang, C. Meng,

H. Qian, H. Wang, M. Dong, Inhibitory effect of Chidamide on the growth of human adenoid cystic carcinoma cells, Biomed. Pharmacother. 99 (2018) 608 - 614.

[18] C.J. Chou, D. Herman, J.M. Gottesfeld, Pimelic diphenylamide 106 is a slow, tight-binding inhibitor of class I histone deacetylases, J. Biol. Chem. 283 (2008) 35402 - 35409.

[19] C. Bonfils, A, Kalita, M. Dubay, L.L. Siu, M.A. Carducci, G. Reid, R.E. Martell, J.M. Besterman, Z. Li, Evaluation of the pharmacodynamic effects of MGCD0103 from preclinical models to human using a novel HDAC enzyme assay, Clin. Cancer Res. 14 (2008) 3441 - 3449.

[20] K.H. Peh, B.Y. Wan, E.S.K. Assem, C.M. Marson, Effect of a selection of histone deacetylase inhibitors on mast cell activation and airway and colonic smooth muscle contraction, Int. Immunopharmacol. 8 (2008) 1793 - 1801.

[21] a) K.J. Dedes, I. Dedes, P. Imesch, A.O. von Bueren, D. Fink, A. Fedier, Acquired vorinostat resistance shows partial cross-resistance to “second-generation” HDAC inhibitors and correlates with loss of histone acetylation and apoptosis but not with altered HDAC and HAT activities, Anti-Cancer Drugs 20 (2009) 321 - 333. b) L. Yanyang, W. Yongzhen, X. Ning, X. Ming, Q. Pengyu, Z. Yanjin, L. Shuxin Li, Design, synthesis and antiproliferative activities of novel benzamides derivatives as HDAC inhibitors, Eur. J. Med. Chem. 100 (2015) 270 - 276. c) B.F.Ayman, A.E. Heba, S.A. Mahmoud, Design, synthesis, and biological evaluation of novel amide and hydrazide based thioether analogs targeting Histone deacteylase (HDAC) enzymes,

Eur. J Med. Chem. 148 (2018) 73 - 85. d) C. Chen, H. Xuben Hou, G. Wang, P. Wenyan, Y. Xinying, Z. Yingkai, F. Hao, Design, synthesis and biological evaluation of quinoline derivatives as HDAC class I inhibitors, Eur. J. Med Chem. 133 (2017) 11 - 23. e) M.M, Charles, J.M. Christopher, S. J. Atkinson, N. Lamadema, N. S. B. Thomas, Potent and Selective Inhibitors of Histone Deacetylase□3 Containing Chiral Oxazoline Capping Groups and a N-(2-Aminophenyl)- benzamide Binding Unit, J. Med. Chem. 58 (2015) 6803 - 6818. f) C. M. Marson, J.M. Christopher, E. Yiannaki, S. J. Atkinson, P. E. Soden, L. Shukla, N. Lamadema , N. S. B. Thomas, Discovery of Potent, Isoform-Selective Inhibitors of Histone Deacetylase Containing Chiral Heterocyclic Capping Groups and a N-(2-Aminophenyl)benzamide Binding Unit, J. Med. Chem. 56 (2013) 56, 6156 - 6174. g) L. Yanyang, W Yongzhen, X. Ning, X. Ming, Q. Pengyu, Z. Yanjin, L. Shuxin. Design, synthesis and antiproliferative activities of novel benzamides derivatives as HDAC inhibitors. Eur. J. Med. Chem.100 (2015) 270 - 276.

[22] a) S. Mehndiratta, Y.L. Hsieh, Y. M Liu, A. W. Wang, H.Y. Lee, L.Y. Liang, S. Kumar, C.M. Teng, C.R. Yang, J.P. Liou, Indole-3-ethylsulfamoylphenylacrylamides: potent histone deacetylase inhibitors with anti-inflammatory activity, Eur. J. Med. Chem. 85 (2014) 468 - 479. b) R. Ojha, H.L. Huang, W.C. HuangFu, Y.W. Wu, K. Nepali, M.J. Lai, C.J. Su, T.Y. Sung, Y.L. Chen, S.L Pan, J.P. Liou, 1-Aroylindoline-hydroxamic acids as anticancer agents, inhibitors of HSP90 and HDAC, Eur. J. Med. Chem. 150 (2018) 667 - 677. c) S. Mehndiratta, R.S. Wang,

H.L. Huang, C.J. Su, C.M. Hsu, Y.W. Wu, S.L. Pan, J.P. Liou, 4-Indolyl-N-hydroxyphenylacrylamides as potent HDAC class I and IIB inhibitors in vitro and in vivo, Eur. J. Med. Chem. 7 (2017) 134:13 - 23. d) K. Nepali, H.Y. Lee, M.J. Lai, R. Ojha, T.Y. Wu, G.X. Wu, M.C. Chen, J.P. Liou, Ring-opened tetrahydro-γ-carbolines display cytotoxicity and selectivity with histone deacetylase isoforms, Eur. J. Med. Chem. 127 (2017) 115-127. e) H.Y. Lee, J.F. Lee, S. Kumar, Y.W. Wu, W.C. HuangFu, M.J. Lai, Y.H. Li, H.L. Huang, F.C.Kuo, C.J. Hsiao, C.C. Cheng, C.R. Yang, J.P. Liou, 3-Aroylindoles display antitumor activity in vitro and in vivo: Effects of N1-substituents on biological activity, Eur. J. Med. Chem. 125 (2017) 1268-1278. f) H.Y. Lee, C.Y. Chang, C.J. Su., H.L. Huang, S. Mehndiratta, Chao Y.H., C.M. Hsu, S.Kumar, T.Y. Sung, Y.Z. Huang, Y.H. Li, C.R. Yang, J.P. Liou, 2-(Phenylsulfonyl)quinoline N-hydroxyacrylamides as potent anticancer agents inhibiting histone deacetylase, Eur. J. Med. Chem. 122 (2016) 92 - 101. g) C.H.Chen, C.H Lee, J.P.Liou, C.M.Teng, S.L.Pan, Molecular mechanisms underlying the antitumor activity of (E)-N-hydroxy-3-(1-(4-methoxyphenylsulfonyl)-1,2,3,4-tetrahydroquinolin-6-yl)acrylamide in human colorectal cancer cells *in vitro* and *in vivo*, Oncotarget 6 (34) (2015) 5991 - 36002. e) Y.M. Liu, H.Y. Lee, M.J. Lai, S.L. Pan, H.L. Huang, F.C, Kuo, M.C.Chen, J.P. Liou, Pyrimidinedione-mediated selective histone deacetylase 6 inhibitors with antitumor activity in colorectal cancer HCT116 cells, Org. Biomol. Chem. 13 (2015) 10226 - 35.

[23] L. Yanyang, W Yongzhen, X. Ning, X. Ming, Q. Pengyu, Z. Yanjin, L. Shuxin, Design, synthesis and antiproliferative activities of novel benzamides derivatives as HDAC inhibitors, Eur. J. Med. Chem. 100 (2015) 270 - 276

[24] a) S. Sharma, J. Singh, R. Ojha, H. Singh, M. Kaur, P.M.S.Bedi, K. Nepali, Design strategies, structure activity relationship and mechanistic insights for purines as kinase inhibitors, Eur. J. Med. Chem. 112 (2016) 298 - 346. b) W. Cheng, Z. Shijun, M. Xiaodong, N. Qiu, P. Peng, R. Sheng, Y. Hu, Design, synthesis and biological evaluation of 6-(nitroimidazole-1Halkyloxyl)-4-anilinoquinazolines as efficient EGFR inhibitors exerting cytotoxic effects both under normoxia and hypoxia, Eur. J. Med.Chem. 89 (2015) 826 - 834.

[25] S. R. Kasibhatla, K. Hong, M. Biamonte, D. J. Busch, P. L. Karjian, J. L. Sensintaffar A. Kamal, R. E. Lough, J. Brekken, K. Lundgren, R. Grecko, G. A. Timony, Y. Ran, R. Mansfield, L. C. Fritz, E. Ulm, F. J. Burrows, M. F. Boehm, Rationally Designed High-Affinity 2-Amino-6-halopurine Heat Shock Protein 90 Inhibitors That Exhibit Potent Antitumor Activity, *J. Med. Chem.* 50 (2007) 12, 2767-277.

[26] B.M. Muller, L. Jana, A. Kasajima, A. Lehmann, J. Prinzler, J. Budczies, K.J. Winzer, M. Dietel, W. Weichert, C. Denkert, Differential expression of histone deacetylases HDAC1, 2 and 3 in human breast cancer--overexpression of HDAC2 and HDAC3 is associated with clinicopathological indicators of disease progression, BMC Cancer, 13 (2013) 215.

[27] R. Buurman, E. Gurlevik, V. Schaffer, M. Eilers, M. Sandbothe, H. Kreipe, L. Wilkens, B. Schlegelberger, F. Kuhnel, B. Skawran, Histone deacetylases activate hepatocyte growth factor signaling by repressing microRNA-449 in hepatocellular carcinoma cells, Gastroenterology, 143 (2012) 811-820 e815.

[28] Y. Zhu, K. Das, J. Wu, M.H. Lee, P. Tan, RNH1 regulation of reactive oxygen species contributes to histone deacetylase inhibitor resistance in gastric cancer cells, Oncogene, 33 (2014) 1527 - 1537.

[29] S. Abou Najem, G. Khawaja, M.H. Hodroj, P. Babikian, S. Rizk, Adjuvant Epigenetic Therapy of Decitabine and Suberoylanilide Hydroxamic Acid Exerts Anti-Neoplastic Effects in Acute Myeloid Leukemia Cells, Cells, 8 (2019).

[30] Z. Liu, K. Ding, L. Li, H. Liu, Y. Wang, C. Liu, R. Fu, A novel histone deacetylase inhibitor Chidamide induces G0/G1 arrest and apoptosis in myelodysplastic syndromes, Biomed. Pharmacother. 83 (2016) 1032-1037.

[31] Z.Q. Ning, Z.B. Li, M.J. Newman, S. Shan, X.H. Wang, D.S. Pan, J. Zhang, M. Dong, X. Du, X.P. Lu, Chidamide (CS055/HBI-8000): a new histone deacetylase inhibitor of the benzamide class with antitumor activity and the ability to enhance immune cell-mediated tumor cell cytotoxicity, Cancer Chemother. Pharmacol. 69 (2012) 901-909.

[32] R.R. Rosato, J.A. Almenara, S. Grant, The histone deacetylase inhibitor MS-275 promotes differentiation or apoptosis in human leukemia cells through a process regulated by generation of reactive oxygen species and induction of p21CIP1/WAF1 1, Cancer Res. 63 (2003) 3637-3645.

[33] G. Silva, B.A. Cardoso, H. Belo, A.M. Almeida, Vorinostat induces apoptosis and differentiation in myeloid malignancies: genetic and molecular mechanisms, PLoS One 8 (2013) e53766.

[34] F. Xu, H. Guo, M. Shi, S. Liu, M. Wei, K. Sun, Y. Chen, A combination of low-dose decitabine and chidamide resulted in synergistic effects on the proliferation and apoptosis of human myeloid leukemia cell lines, Am. J. Transl. Res. 11 (2019) 7644-7655.

[35] S.A. Amin, S. Bhargava, N. Adhikari, S. Gayen, T. Jha, Exploring pyrazolo[3,4-d]pyrimidine phosphodiesterase 1 (PDE1) inhibitors: a predictive approach combining comparative validated multiple molecular modelling techniques, J. Biomol. Struct. Dyn. 36 (2018) 590-608.

[36] S.A. Amin, P. Bhattacharya, S. Basak, S. Gayen, A. Nandy, A. Saha, Pharmacoinformatics study of Piperolactam A from Piper betle root as new lead for non steroidal anti fertility drug development, Comput. Biol. Chem. 67 (2017) 213-224.

[37] K. Chen, L. Xu, O. Wiest, Computational exploration of zinc binding groups for HDAC inhibition, J. Org. Chem. 78 (2013) 5051 - 5055.

[38] L. Zhang, J. Zhang, Q. Jiang, L. Zhang, W. Song, Zinc binding groups for histone deacetylase inhibitors, J. Enzyme. Inhib. Med. Chem. 33 (2018) 714 - 721.

[39] F. Cao, M.R.H. Zwinderman, F.J. Dekker, The Process and Strategy for Developing Selective Histone Deacetylase 3 Inhibitors, Molecules 23 (2018) pii: E551.

[40] S. Kalyaanamoorthy, Y.P. Chen, Energy based pharmacophore mapping of HDAC inhibitors against class I HDAC enzymes, Biochim. Biophys. Acta 1834 (2013) 317 - 328.

[41] M.J. Bottomley, P. Lo Surdo, P. Di Giovine, A. Cirillo, R. Scarpelli, F. Ferrigno, P. Jones, P. Neddermann, R. De Francesco, C. Steinkühler, P. Gallinari, A. Carfí, Structural and functional analysis of the human HDAC4 catalytic domain reveals a regulatory structural zinc-binding domain, J. Biol. Chem. 283 (2008) 26694 - 26704.

[42] T.A. Miller, D.J. Witter, S. Belvedere, Histone deacetylase inhibitors, J. Med. Chem. 46 (2003) 5097 - 5116.

[43] K. Krennhrubec, B.L. Marshall, M. Hedglin, E, Verdin, S.M. Ulrich, Design and evaluation of 'Linkerless' hydroxamic acids as selective HDAC8 inhibitors, Bioorg. Med. Chem. Lett 17 (2007) 2874 - 2878.

[44] K.N. Hassell, Histone Deacetylases and their Inhibitors in Cancer Epigenetics, Diseases, 7 (2019).

[45] E. Seto, M. Yoshida, Erasers of histone acetylation: the histone deacetylase enzymes, Cold Spring Harb. Perspect. Biol. 6 (2014) a018713.

[46] M.A. Deardorff, M. Bando, R. Nakato, E. Watrin, T. Itoh, M. Minamino, K. Saitoh, M. Komata, Y. Katou, D. Clark, K.E. Cole, E. De Baere, C. Decroos, N. Di Donato, S. Ernst, L.J. Francey, Y. Gyftodimou, K. Hirashima, M. Hullings, Y. Ishikawa, C. Jaulin, M. Kaur, T. Kiyono, P.M. Lombardi, L. Magnaghi-Jaulin, G.R. Mortier, N. Nozaki, M.B. Petersen, H. Seimiya, V.M. Siu, Y. Suzuki, K. Takagaki, J.J. Wilde, P.J. Willems, C. Prigent, G. Gillessen-Kaesbach, D.W. Christianson, F.J. Kaiser, L.G. Jackson, T. Hirota, I.D. Krantz, K. Shirahige, HDAC8 mutations in Cornelia de Lange syndrome affect the cohesin acetylation cycle, Nature, 489 (2012) 313-317.

[47] C. Hubbert, A. Guardiola, R. Shao, Y. Kawaguchi, A. Ito, A. Nixon, M. Yoshida, X.F. Wang, T.P. Yao, HDAC6 is a microtubule-associated deacetylase, Nature, 417 (2002) 455-458.

[48] Y. Li, E. Seto, HDACs and HDAC Inhibitors in Cancer Development and Therapy, Cold Spring Harb. Perspect. Med. 6 (2016).

[49] P. Chun, Histone deacetylase inhibitors in hematological malignancies and solid tumors, Arch. Pharm. Res. 38 (2015) 933-949.

[50] S. Liu, H. Cheng, W. Kwan, J.M. Lubieniecka, T.O. Nielsen, Histone deacetylase inhibitors induce growth arrest, apoptosis, and differentiation in clear cell sarcoma models, Mol. Cancer Ther. 7 (2008) 1751-1761.

[51] T. Yamaguchi, F. Cubizolles, Y. Zhang, N. Reichert, H. Kohler, C. Seiser, P. Matthias, Histone deacetylases 1 and 2 act in concert to promote the G1-to-S progression, Genes Dev. 24 (2010) 455-469.

[52] G. Zupkovitz, R. Grausenburger, R. Brunmeir, S. Senese, J. Tischler, J. Jurkin, M. Rembold, D. Meunier, G. Egger, S. Lagger, S. Chiocca, F. Propst, G. Weitzer, C. Seiser, The cyclin-dependent kinase inhibitor p21 is a crucial target for histone deacetylase 1 as a regulator of cellular proliferation, Mol. Cell. Biol. 30 (2010) 1171-1181.

[53] A.G. Georgakilas, O.A. Martin, W.M. Bonner, p21: A Two-Faced Genome Guardian, Trends Mol. Med. 23 (2017) 310-319.

[54] J. Sonnemann, C. Marx, S. Becker, S. Wittig, C.D. Palani, O.H. Kramer, J.F. Beck, p53-dependent and p53-independent anticancer effects of different histone deacetylase inhibitors, Br. J. Cancer 110 (2014) 656-667.

[55] P. Fedele, O. Laura, S. Cinieri, Targeting triple negative breast cancer with histone deacetylase inhibitors, Expert Opin. Investig. Drugs. 26 (2017) 1199-1206.

[56] LeadIT, B. http://www. biosolveit. de/LeadIT. *accessed 12th Jan* (2019).

[57] S.K. Burley, H.M. Berman, C. Bhikadiya, C. Bi, L. Chen, L. Di Costanzo, C. Christie, K. Dalenberg, J.M. Duarte, S. Dutta, Z. Feng Z, S. Ghosh S, D.S. Goodsell, R.K. Green, V. Guranovic, D. Guzenko, B.P. Hudson, T. Kalro, Y. Liang, R. Lowe, H. Namkoong, E. Peisach, I. Periskova, A. Prlic, C. Randle, A. Rose, P. Rose, R. Sala, M. Sekharan, C. Shao, L. Tan, Y.P. Tao, Y. Valasatava, M. Voigt, J. Westbrook, J. Woo, H. Yang, J. Young, M. Zhuravleva, C. Zardecki C, RCSB Protein Data Bank: biological macromolecular structures enabling research and education in fundamental biology, biomedicine, biotechnology and energy, Nucleic Acids Res. **47** (2019) D464 - D474.

[58] W.A. Warr, Scientific workflow systems: Pipeline Pilot and KNIME, J. Comput. Aided Mol. Des. 26 (2012) 801-804.

Figure Captions

Fig. 1. Structures of clinically approved HDAC inhibitors

Fig. 2. Design strategy and structures of the designed compounds (**7**-**18**)

Fig. 3. Cytotoxicity of 14, MS-275 (**5**) and Chidamide (**6**) in breast cancer cell lines. Three cell lines were treated with a series of concentration of the indicated compounds and cell viability was determined by MTT assay. The concentration (μM) inhibiting 50% of cell growth (IC_{50}) was calculated by CompuSyn software. Results are displayed as mean ± S.D. from three independent experiments (n≥9). An unpaired Mann-Whitney test was used for statistical analysis. ***p<0.001; ****p<0.0001.

Fig. 4. Cytotoxicity of SAHA (**1**), **14**, MS-275 (**5**) and Chidamide (**6**) in leukemia cell lines. Three cell lines were treated with a series of concentration of the indicated compounds and cell viability was determined by MTS assay. The concentration (μM) inhibiting 50% of cell growth (IC_{50}) was calculated by CompuSyn software and displayed as mean ± S.D. from three independent experiments (n=9). An unpaired Mann-Whitney test was used for statistical analysis. ***p<0.001; ****p<0.0001.

Fig. 5. The binding poses of compound **14** in HDAC1-3. Compound **14** docked in the active site of HDAC1-3. The ZBG (1), linker (2), cap group (3) and residues are labeled as shown. Hydrogen bonds and zinc coordination is labeled as dash green lines.

Fig. 6. The binding pose of compound **14** in HDAC isozymes. The binding pose of Compound **14** (yellow) in HDAC1 (pink) is superimposed onto (A) HDAC4 (green), (B) HDAC6 (orange) and (C) HDAC8 (blue). Residues in the active site that differ are labeled as shown. Hydrogen bonds are denoted as dashed green lines.

Fig. 7. Molecular dynamics (MD) simulation of compound **14** in HDAC1. (A) The conformation pose of Compound **14** at the end of the simulation. (B) The docking pose (yellow) and the final MD simulation pose (blue) were superimposed. Similar pose was observed. (C) The interaction fraction of HDAC1 active residues.

Fig. 8. MS-275 (**5**), **16** and **14** elevate acetylation level of histone H3 and expression of p21. (A) MDA-MB-231 cells were treated with the indicated compounds for 24 hours. Cell lysates were harvested and subjected to western blotting analysis for the indicated acetylation levels on lysine 9 of histone H3 (ac-H3 K9), lysine 5/8/12/16 of histone H4 (ac-H4 K5/8/12/16), lysine 40 of α-tubulin (ac-α-tubulin K40) and lysine 105/106 of SMC3 (ac-SMC3 K105/106). (B) Acetylation level of H3 K9 in MDA-MB-231 cells treated with 2 μM of the indicated compounds was quantified by MultiGauge software. Results are displayed as mean ± S.D. from three independent experiments (n= 3).

Fig. 9. MS-275 (**5**), **16** and **14** arrest cell cycle in G_1 and trigger apoptosis. (A) MDA-MB-231 cells were treated with 4 μM of the indicated compounds for 24 hours, follow by incubation with or without nocodazole for 10 hours to trap cells in mitosis. Cell cycle progression was analyzed

by flow cytometry. (B) MDA-MB-231 cells were treated with 16 μM of the indicated compounds for 48 hours, followed by cell cycle progression analysis with flow cytometry. Percentage of sub-G_1 population was calculated by FlowJo software. (C) MDA-MB-231 cells treated with the indicated compounds were subjected to western blotting analysis for the indicated caspase targets. The protein level of α-tubulin was used as the loading control.

Fig. 10. Antitumor efficacy of compound **14** in human MDA-MB-231 breast cancer xenograft model. BALB/c nude mice were injected subcutaneously with MDA-MB-231 cells and treated for 10 mg/kg Taxol, 25 mg/ml or 50 mg/ml compound **14** after tumors reached about 80-100 mm^3. Tumor volume (A) and body weight (B) were monitored twice weekly. IV: intravenous injection; IP: intraperitoneal injection; QOD: every other day; QD: every day; TGI: tumor growth inhibition.

Fig. 11. Summarized representation of the results

Table 1. Antiproliferative activity of compounds against human cancer cell lines

Compounds	**MDA-MB-231 Breast**	**HepG2 Liver**
	IC_{50} (μM)	
7	>8	>8
8	3.24 ± 0.39	>8
9	>8	>8
10	4.64 ± 0.12	5.55 ± 0.28
11	7.65 ± 0.55	>8
12	>8	>8
13	3.08 ± 0.14	4.41 ± 1.49
14	1.48 ± 0.06	2.44 ± 0.18
15	3.17 ± 0.11	4.20 ± 0.50
16	5.32 ± 0.13	4.85 ± 1.81
17	3.78 ± 0.30	4.21 ± 0.51
18	>8	>8
MS-275, 5	2.60 ± 0.16	4.54 ± 0.21
Chidamide, 6	3.60 ± 0.36	>8

Table. 2 HDAC inhibition activity and isoform selectivity of compounds and reference **5**.

Compounds	HDAC1	HDAC2	HDAC6	HDAC8
	IC_{50} (M)[a]			
8	6.85×10^{-7}	3.78×10^{-6}	$> 10^{-5}$	$> 10^{-5}$
9	1.82×10^{-7}	1.45×10^{-6}	1.13×10^{-8}	3.52×10^{-7}
10	1.65×10^{-7}	7.39×10^{-7}	$> 10^{-5}$	$> 10^{-5}$
11	8.62×10^{-7}	6.51×10^{-6}	$> 10^{-5}$	$> 10^{-5}$
13	2.71×10^{-7}	7.61×10^{-7}	$> 10^{-5}$	$> 10^{-5}$
14	1.08×10^{-7}	5.85×10^{-7}	$> 10^{-5}$	6.81×10^{-6}
15	2.39×10^{-8}	1.79×10^{-7}	$> 10^{-5}$	9.61×10^{-6}
16	9.33×10^{-8}	1.46×10^{-6}	$> 10^{-5}$	$> 10^{-5}$
17	1.23×10^{-6}	1.15×10^{-6}	$> 10^{-5}$	$> 10^{-5}$
MS275, **5**	5.44×10^{-7}	6.13×10^{-7}	$> 10^{-5}$	9.88×10^{-6}

[a]These assays were conducted by the Reaction Biology Corporation, Malvern, PA. All compounds were dissolved in DMSO and tested in 10-dose IC_{50} mode with 3-fold serial dilution starting at 10 μM.

Table. 3 HDAC inhibition Activity of compounds **14**, **15** and reference **5**

	HDAC1	HDAC2	HDAC3	HDAC4	HDAC5	HDAC6	HDAC7	HDAC8	HDAC9	HDAC10
Compds					IC_{50} (μM)[a]					
14	0.108	0.585	0.563	> 10	> 10	> 10	> 10	6.81	> 10	5.75
15	0.023	0.179	0.245	-	-	ND	-	ND	-	ND
5	0.544	0.613	0.624	> 10	> 10	> 10	> 10	9.88	> 10	3.15

[a]These assays were conducted by the Reaction Biology Corporation, Malvern, PA. All compounds were dissolved in DMSO and tested in 10-dose IC_{50} mode with 3-fold serial dilution starting at 10 μM.

- Empty cells indicate no inhibition or compound activity that could not be fit to an IC_{50} curve

Table 4. Antiproliferative activity of compounds against HDACi sensitive or resistant cells

Compounds	**YCC11 (HDACi-sensitive)**	**YCC3/7 (HDACi-resistant)**
	IC_{50} (μM)	
8	9.85 ± 0.35	10.10 ± 0.75
10	6.26 ± 1.01	14.38 ± 0.10
11	16.59 ± 1.39	>32
13	7.06 ± 0.43	15.37 ± 0.11
14	4.77 ± 0.29	4.79 ± 0.37
15	24.65 ± 1.10	30.41 ± 3.32
16	9.27 ± 0.27	12.16 ± 0.31
17	4.67 ± 0.38	12.28 ± 1.03
MS-275, 5	6.03 ± 0.44	12.98 ± 1.02
Chidamide, 6	17.07 ± 1.60	20.44 ± 0.38

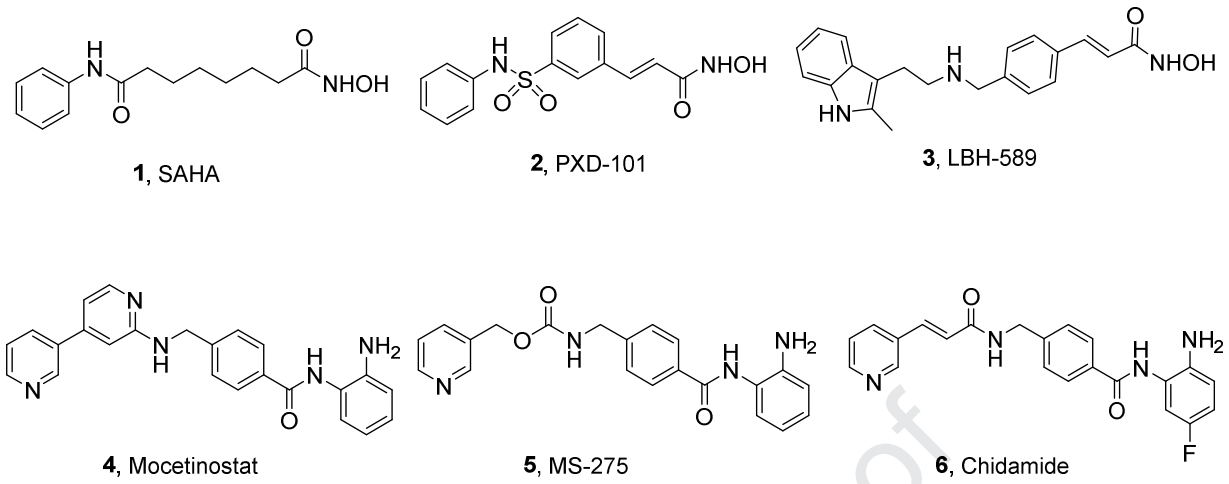

Fig. 1. Structures of HDAC inhibitors

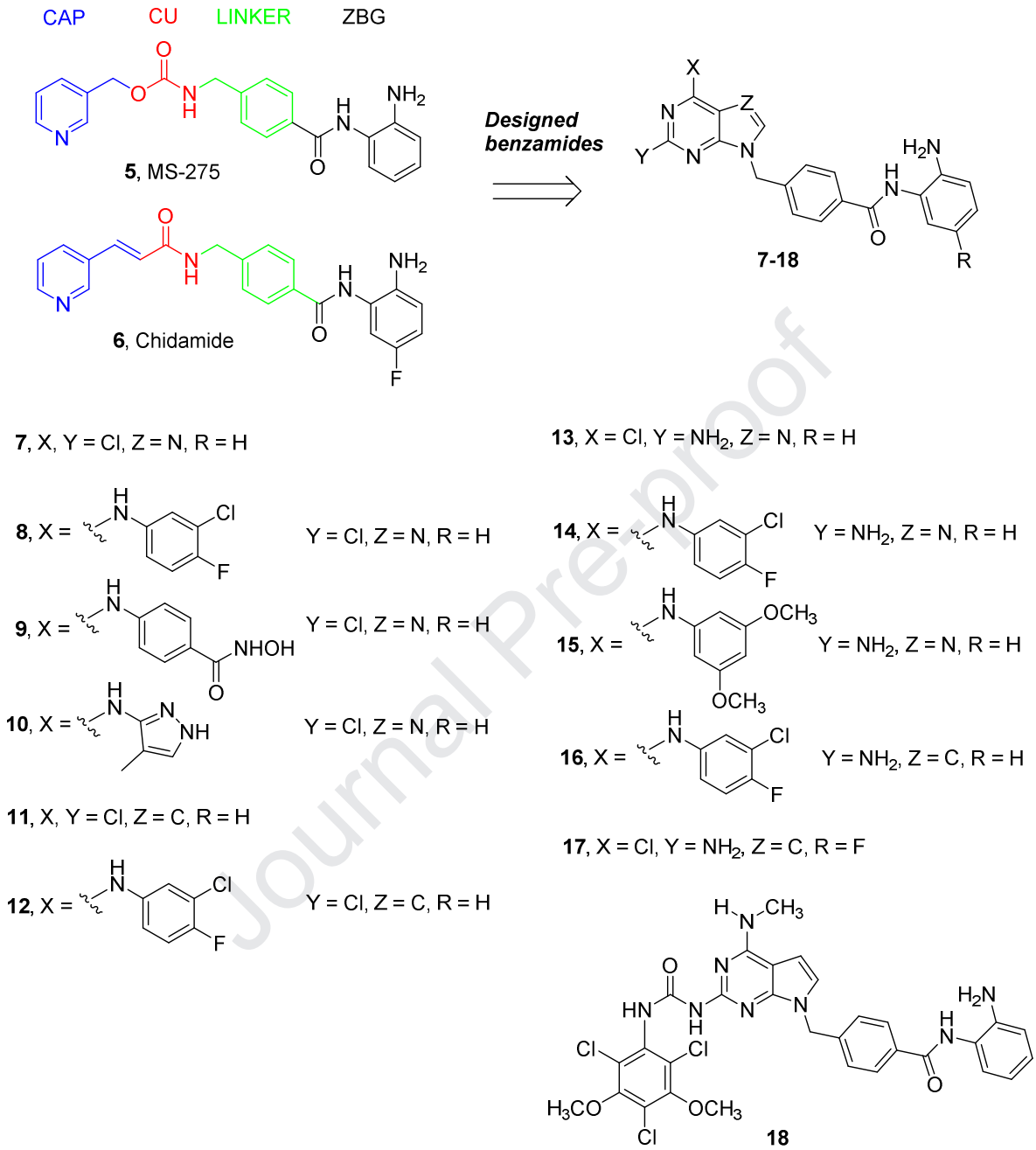

Fig. 2. Design strategy and structures of the designed compounds (**7-18**)

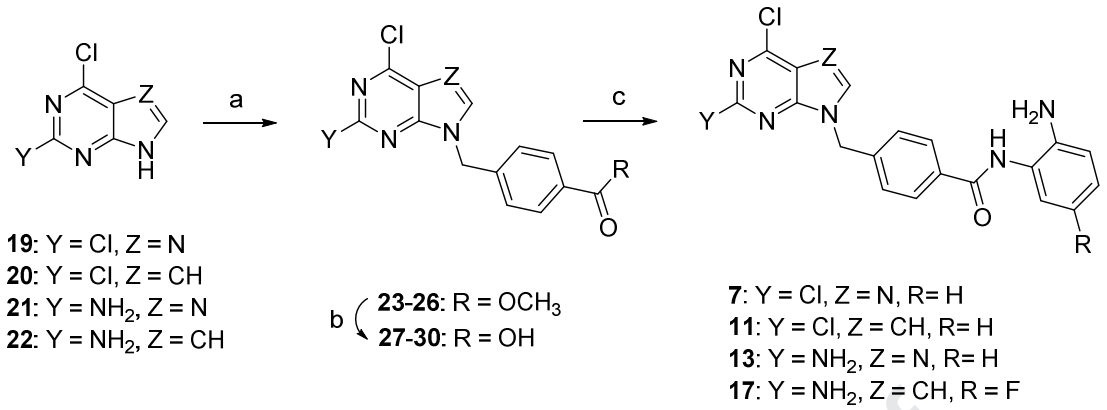

Scheme 1. Reagents and conditions a) Methyl 4-(bromomethyl)benzoate, K_2CO_3, DMF, 60 ^oC; b) i) LiOH, dioxane, rt; c) benzene-1,2-diamine, EDC, HOBt, DIPEA, DMF,rt; For compound **17** i) (2-Amino-4-fluoro-phenyl)-carbamic acid *tert*-butyl ester, EDC, HOBt, DIPEA, DMF, rt; ii) CF_3COOH, CH_2Cl_2, rt.

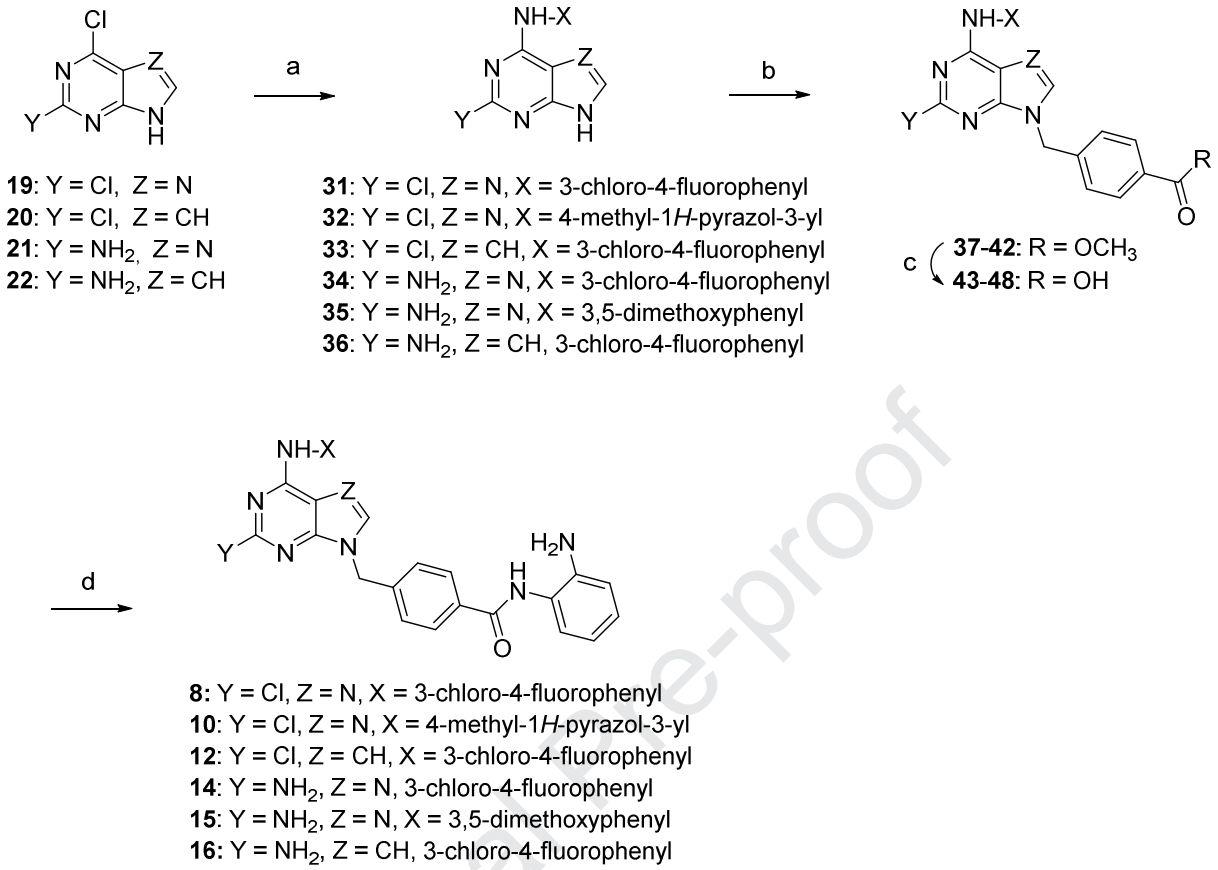

Scheme 2. Reagents and conditions a) appropriate amines, conc. HCl, isopropanol, reflux; b) Methyl 4-(bromomethyl)benzoate, K_2CO_3, DMF, 60 ^oC; c) LiOH, dioxane, rt; d) benzene-1,2-diamine, EDC, HOBt, DIPEA, DMF, rt.

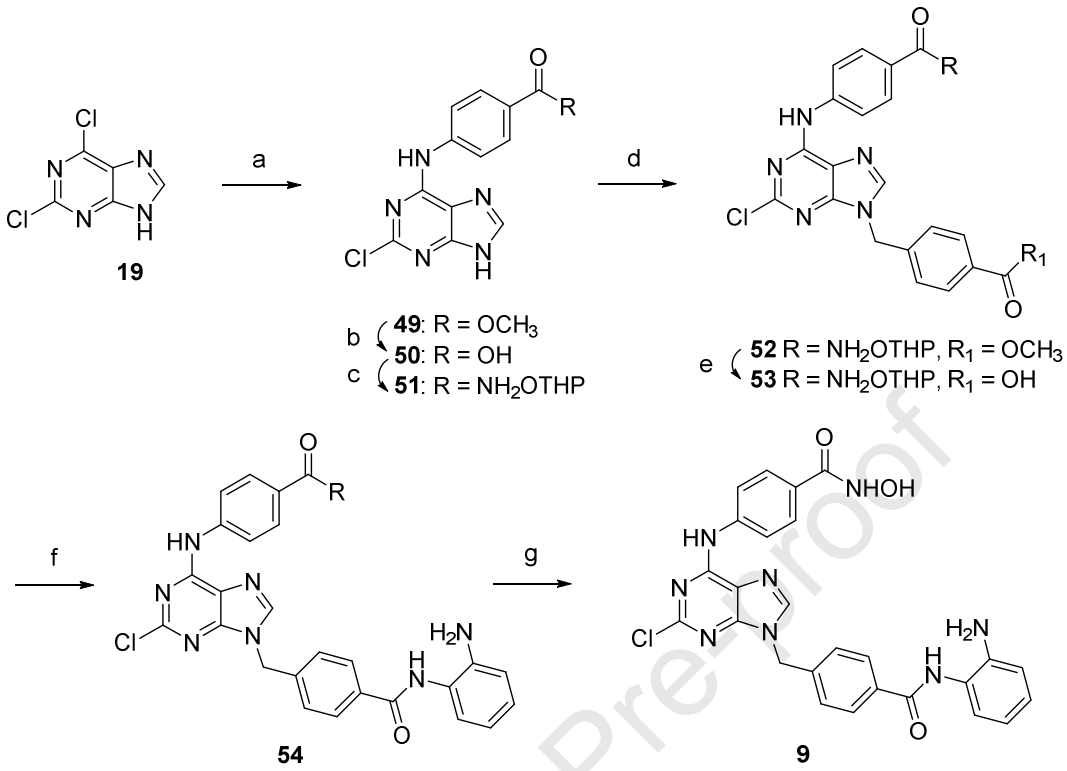

Scheme 3. Reagents and conditions a) Methyl 4-aminobenzoate, conc. HCl, isopropanol, reflux; b) LiOH, dioxane, rt; c) NH_2OTHP, EDC, HOBT, DIPEA, DMF, rt; d) Methyl 4-(bromomethyl)benzoate, K_2CO_3, DMF, 60 ^oC; e) LiOH, dioxane, rt; f) benzene-1,2-diamine, EDC, HOBT, DIPEA, DMF, rt; g) CF_3COOH, CH_3OH, rt.

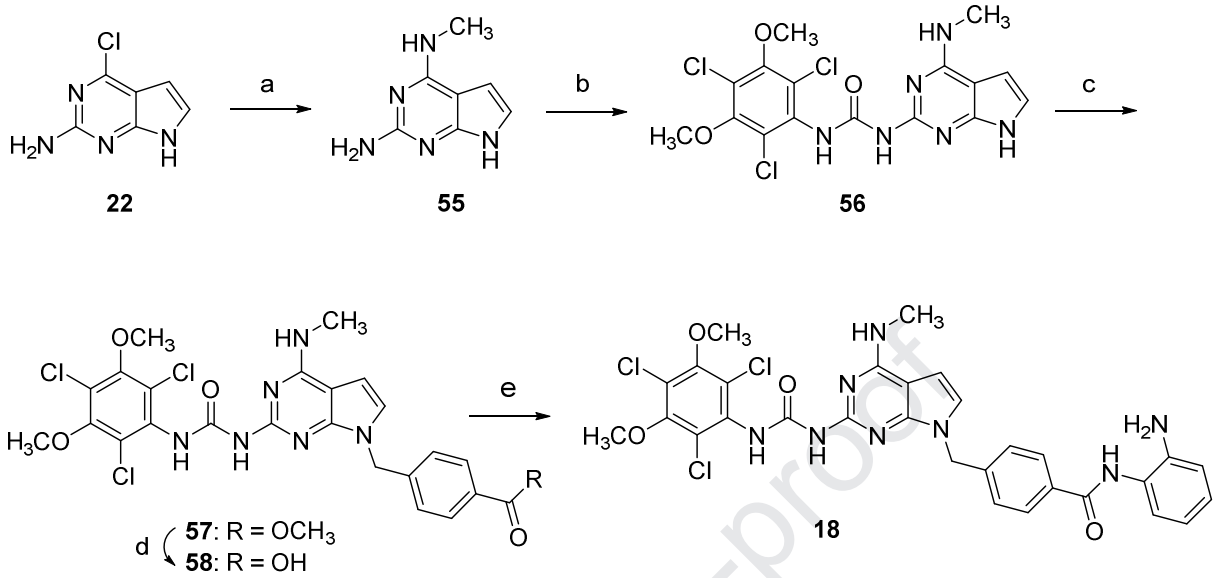

Scheme 4. Reagents and conditions a) Methylamine, butanol, 70 ^{o}C; b) i) triphosgene, THF, rt; ii) 2,4,6-trichloro-3,5-dimethoxyaniline. toluene, reflux; c) methyl 4-(bromomethyl)benzoate. K_2CO_3, DMF, 60 ^{o}C, d) LiOH, dioxane, rt; e) benzene-1,2-diamine, EDC, HOBT, DIPEA, DMF, rt.

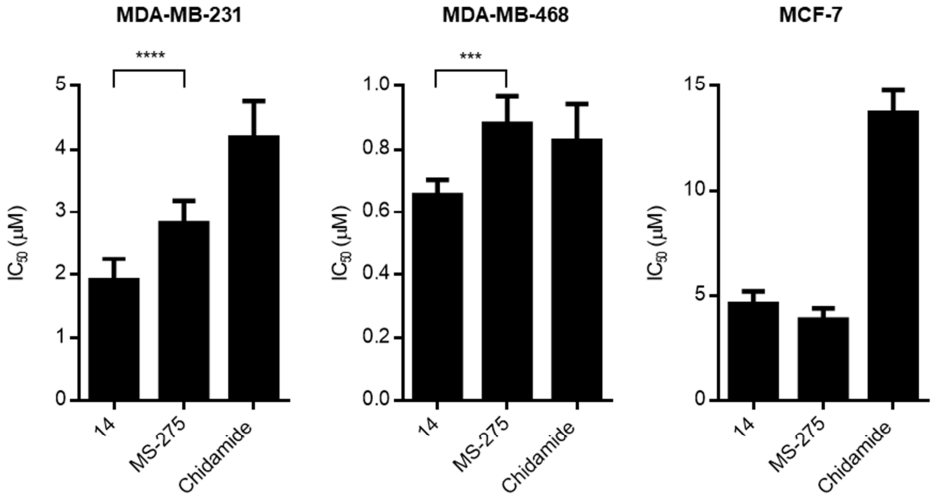

Fig. 3. Cytotoxicity of **14**, MS-275 (**5**) and Chidamide (**6**) in breast cancer cell lines. Three cell lines were treated with a series of concentration of the indicated compounds and cell viability was determined by MTT assay. The concentration (μM) inhibiting 50% of cell growth (IC_{50}) was calculated by CompuSyn software. Results are displayed as mean ± S.D. from three independent experiments (n≥9). An unpaired Mann-Whitney test was used for statistical analysis. ***p<0.001; ****p<0.0001.

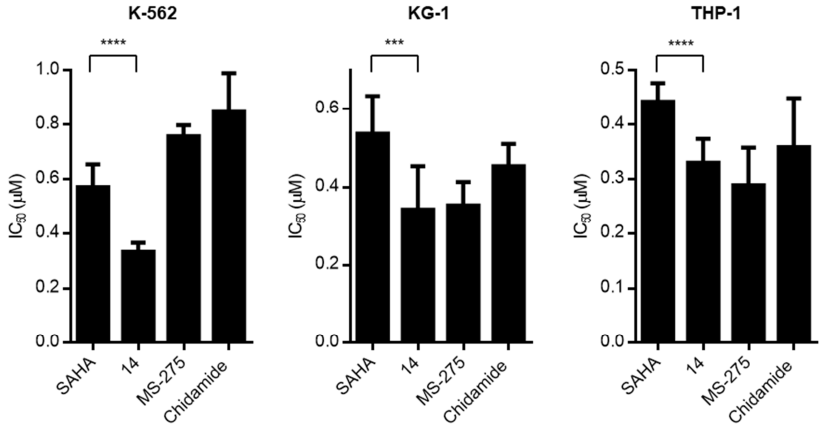

Fig. 4. Cytotoxicity of SAHA (**1**), **14**, MS-275 (**5**) and Chidamide (**6**) in leukemia cell lines. Three cell lines were treated with a series of concentration of the indicated compounds and cell viability was determined by MTS assay. The concentration (μM) inhibiting 50% of cell growth (IC_{50}) was calculated by CompuSyn software and displayed as mean ± S.D. from three independent experiments (n=9). An unpaired Mann-Whitney test was used for statistical analysis. ***p<0.001; ****p<0.0001.

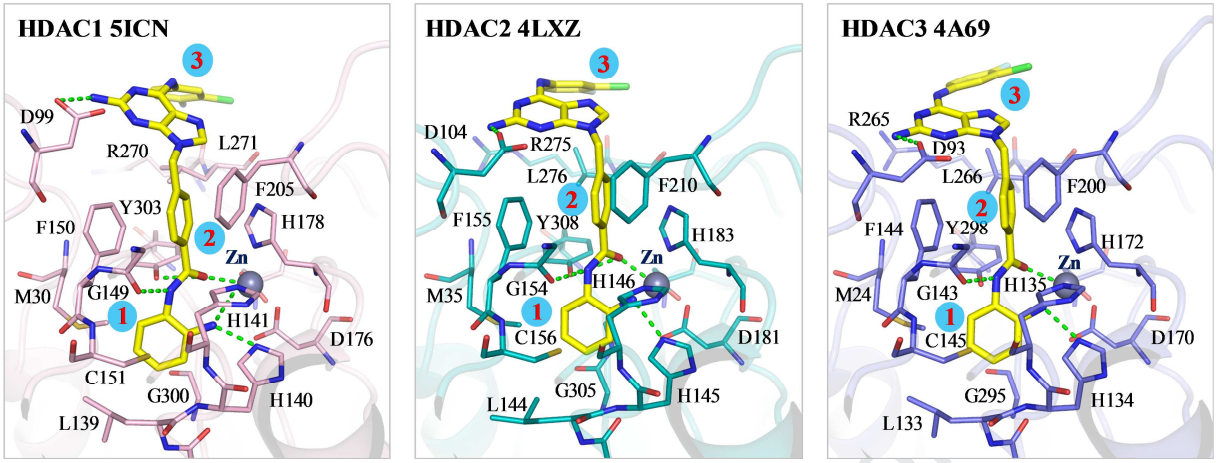

Fig. 5. The binding poses of compound **14** in HDAC1-3. Compound **14** docked in the active site of HDAC1-3. The ZBG (1), linker (2), cap group (3) and residues are labeled as shown. Hydrogen bonds and zinc coordination is labeled as dash green lines.

(A) (B) (C)

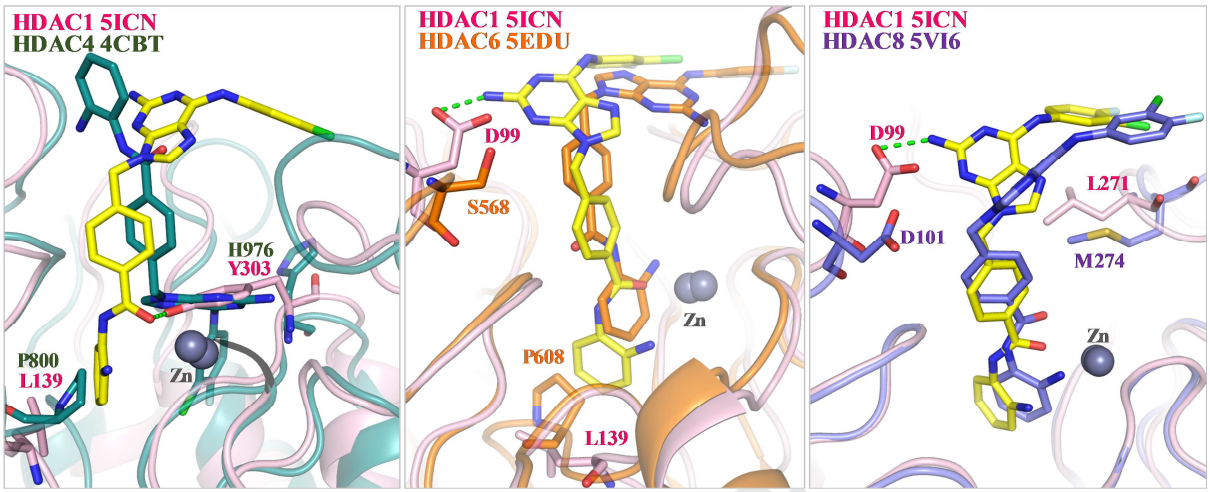

Fig. 6. The binding pose of compound **14** in HDAC isozymes. The binding pose of compound **14** (yellow) in HDAC1 (pink) is superimposed onto (A) HDAC4 (green), (B) HDAC6 (orange) and (C) HDAC8 (blue). Residues in the active site that differ are labeled as shown. Hydrogen bonds are denoted as dashed green lines.

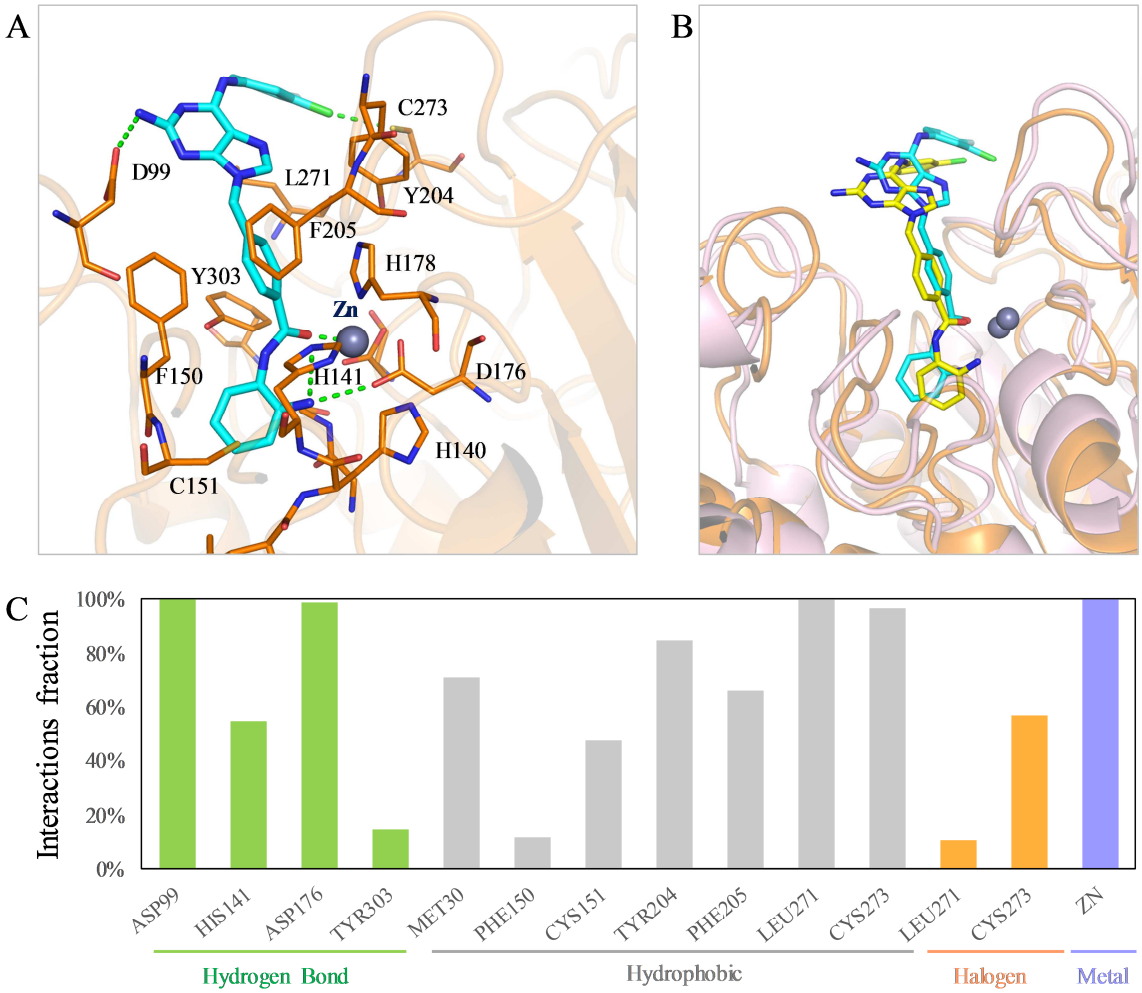

Fig. 7. Molecular dynamics (MD) simulation of compound **14** in HDAC1. (A) The conformation pose of Compound **14** at the end of the simulation. (B) The docking pose (yellow) and the final MD simulation pose (blue) were superimposed. Similar pose was observed. (C) The interaction fraction of HDAC1 active residues.

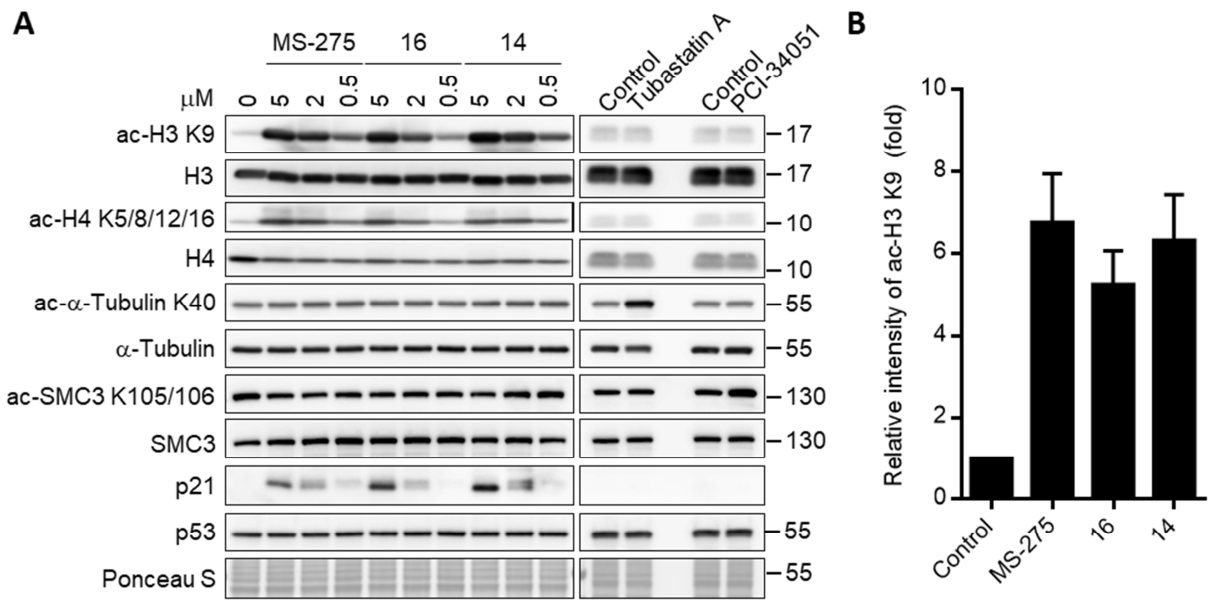

Fig. 8. MS-275 (**5**), **16** and **14** elevate acetylation level of histone H3 and expression of p21. (A) MDA-MB-231 cells were treated with the indicated compounds for 24 hours. Cell lysates were harvested and subjected to western blotting analysis for the indicated acetylation levels on lysine 9 of histone H3 (ac-H3 K9), lysine 5/8/12/16 of histone H4 (ac-H4 K5/8/12/16), lysine 40 of α-tubulin (ac-α-tubulin K40) and lysine 105/106 of SMC3 (ac-SMC3 K105/106). (B) Acetylation level of H3 K9 in MDA-MB-231 cells treated with 2 μM of the indicated compounds was quantified by MultiGauge software. Results are displayed as mean ± S.D. from three independent experiments (n= 3).

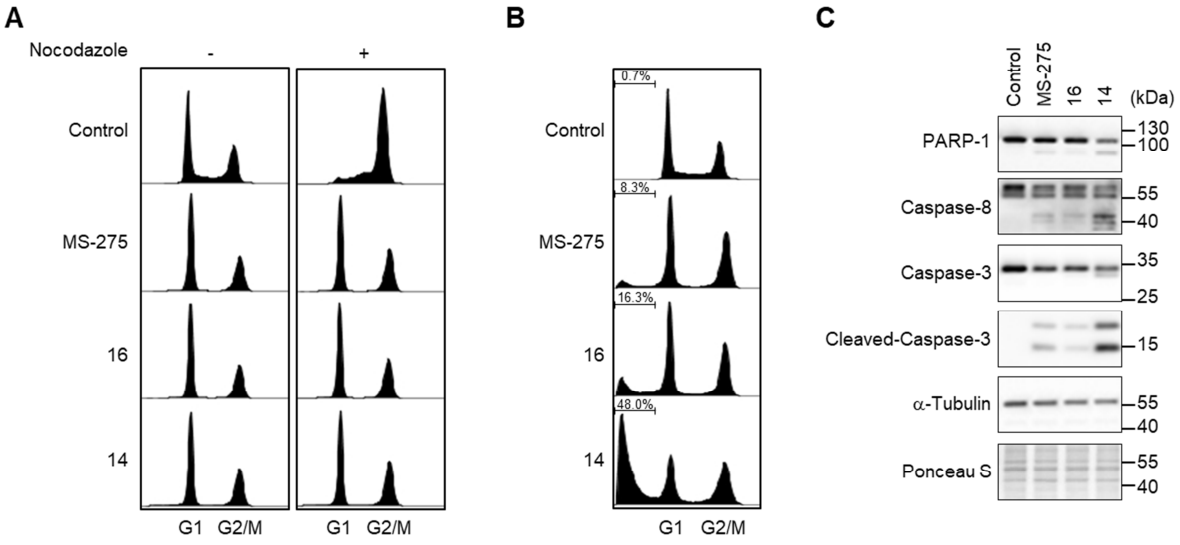

Fig. 9. MS-275 (**5**), **16** and **14** arrest cell cycle in G_1 and trigger apoptosis. (A) MDA-MB-231 cells were treated with 4 μM of the indicated compounds for 24 hours, followed by incubation with or without nocodazole for 10 hours to trap cells in mitosis. Cell cycle progression was analyzed by flow cytometry. (B) MDA-MB-231 cells were treated with 16 μM of the indicated compounds for 48 hours, followed by cell cycle progression analysis with flow cytometry. Percentage of sub-G_1 population was calculated by FlowJo software. (C) MDA-MB-231 cells treated with the indicated compounds were subjected to Western blotting analysis for the indicated caspase targets. The protein level of α-Tubulin was used as the loading control.

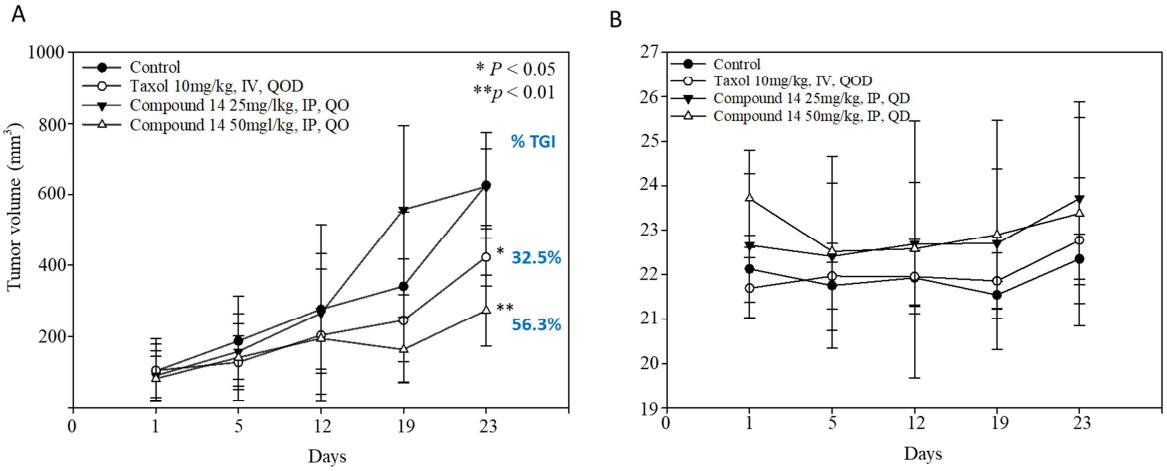

Fig. 10. Antitumor efficacy of compound **14** in human MDA-MB-231 breast cancer xenograft model. BALB/c nude mice were injected subcutaneously with MDA-MB-231 cells and treated for 10 mg/kg Taxol, 25 mg/ml or 50 mg/ml compound **14** after tumors reached about 80-100 mm^3. Tumor volume (A) and body weight (B) were monitored twice weekly. IV: intravenous injection; IP: intraperitoneal injection; QOD: every other day; QD: every day; TGI: tumor growth inhibition.

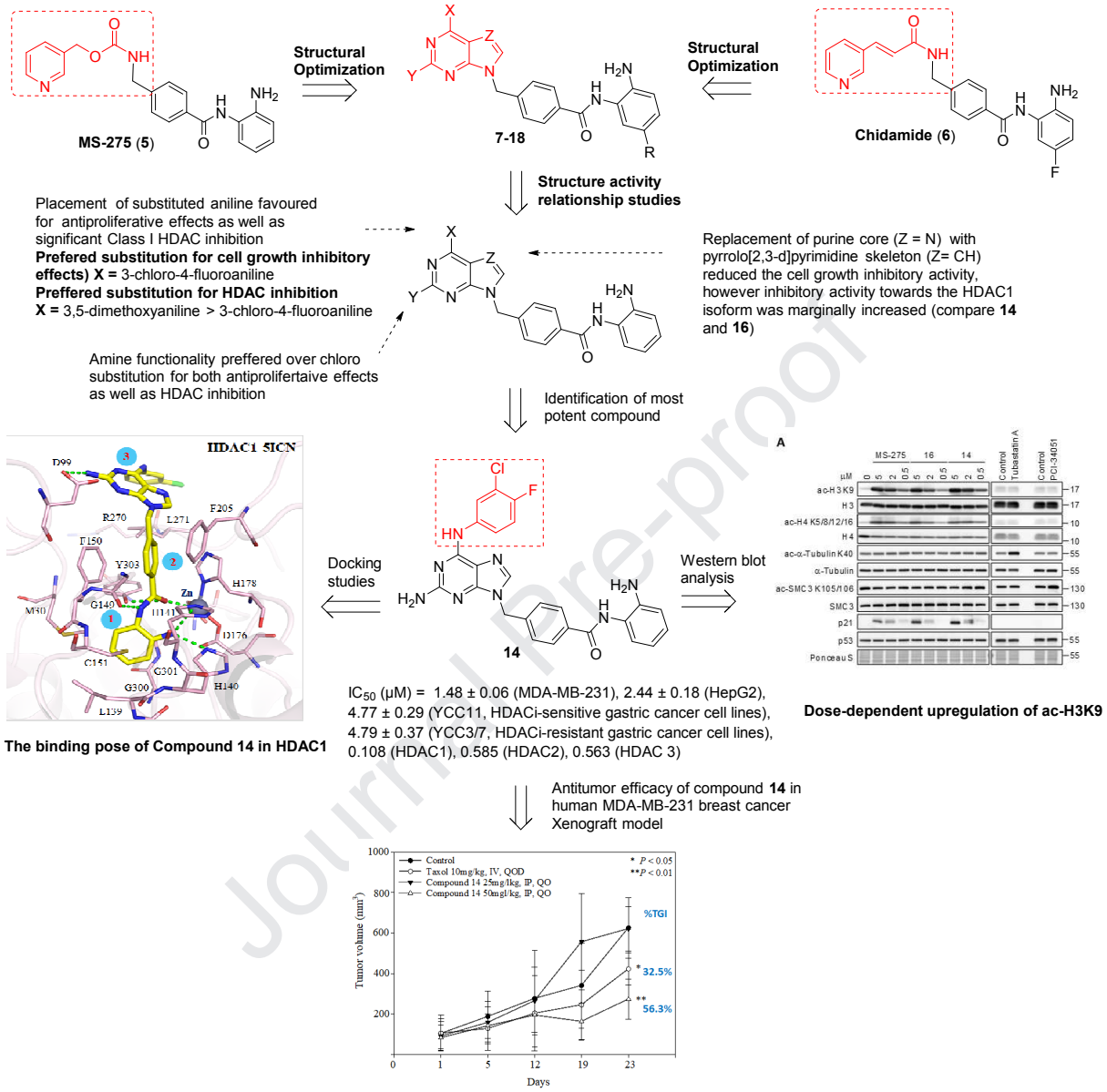

Fig. 11. Summarized representation of the results

Research highlights

1. A series of benzamides containing purine/purine isoster as capping group has been synthesized.

2. Benzamide **14** was found to be virulent in YCC3/7 cell line (HDAC resistant gastric cell line).

3. Benzamide **14** remarkably suppressed the growth of triple negative breast cancer cell lines

4. Benzamide **14** displayed striking inhibitory effects towards HDAC 1, 2 and 3 isoforms more pronounced than MS-275.

5. Benzamide **14** also exerts a dose-dependent upregulation of ac-H3K9 in MDA-MB-231 cells, triggers cell cycle arrest in G1 phase

Declaration of interests

☒ The authors declare that they have no known competing financial interests or personal relationships that could have appeared to influence the work reported in this paper.

☐The authors declare the following financial interests/personal relationships which may be considered as potential competing interests: